2018-01-01

Assessing Performance Of Detectors Of High Frequency Oscillations In Eeg Signals

Deeksha Seetharama Bhat
University of Texas at El Paso, deeksha.bhat765@gmail.com

ASSESSING PERFORMANCE OF DETECTORS OF HIGH FREQUENCY OSCILLATIONS IN EEG SIGNALS

DEEKSHA SEETHARAMA BHAT

Master's Program in Electrical Engineering

APPROVED:

Sergio Cabrera, Ph.D., Chair

Rodrigo Romero, Ph.D., Co-Chair

Olac Fuentes, Ph.D.

Stephen Sands, Ph.D.

Charles Ambler, Ph.D.
Dean of the Graduate School

ASSESSING PERFORMANCE OF DETECTORS OF HIGH FREQUENCY OSCILLATIONS IN EEG SIGNALS

by

DEEKSHA SEETHARAMA BHAT,B.E

THESIS

Presented to the Faculty of the Graduate School of

The University of Texas at El Paso

in Partial Fulfillment

of the Requirements

for the Degree of

MASTER OF SCIENCE

Department of Electrical and Computer Engineering

THE UNIVERSITY OF TEXAS AT EL PASO

December 2018

Acknowledgements

I would like to Thank Dr. Sergio D Cabrera, Dr. Rodrigo A Romero and Dr. Stephen F. Sands for guiding me throughout my work. I also take this opportunity to Thank my parents for their sacrifice and support in providing best education possible and my friends for supporting and helping me to get till here. I also acknowledge support from the Texas Instruments Foundation Endowed Scholarship Program during several semesters before and during 2018.

Abstract

Attempts to perform epileptic seizure prediction have been made for decades, but there is no solution yet that is generally effective, though some progress in this area has been reported. Interictal epileptic spikes were considered as the only biomarkers of seizure-generating brain tissue until the recent discovery of high-frequency oscillations (HFOs) in electroencephalographic (EEG) signals, with frequency contents in the range from 80 Hz to 800 Hz. HFOs are now considered as biomarkers of epileptogenic tissue and the seizure onset zone. However, there are challenges in the definition and detection of HFO events which complicate this perspective. In studies about automatic HFO detection in EEG recordings, visual markings of HFOs by experts are considered as gold standards to compare the performance of detection algorithms. However different authors define their gold standards in variable manners and HFO detection methods are used to produce candidate HFOs which must be further classified visually to declare them as true HFO events. Likewise, when comparing automatic detectors, only HFO rates per unit time are noted without a detailed analysis of candidate vs true HFO events. Also, there is no consistent method as to whether all or some part of such events must be considered for a given analysis. This work correlates events detected with different automatic detectors independently of any detection by experts and analyzes the effect and potential benefit of performance differences in automatic detectors. It also briefly analyzes the possibilities and options for using multiple HFO detectors together. Results show that combination of detectors gives better performance than the individual detectors.

Table of Contents

List of Tables

List of Figures

Chapter 1

Introduction

Epilepsy is a neurological disorder characterized by unpredicted unprovoked repetitive seizures. Seizures are sudden changes in electrical activity of the epileptic brain that affect body movements, sensation and feeling. Almost 1% of the world population is affected by epilepsy (Gloss D et al., 2014, Mormann et al.,2007). The initial treatment recommended for epilepsy is antiepileptic drugs (AED), which control seizures. This is successful in about 60-80% of the patients. In the worst case, i.e. in drug-resistant patients, resective surgery of brain epileptogenic tissue is considered with an aim to completely eliminate epilepsy. However, only about 10% of patients benefit from surgery. Remaining patients must suffer with epilepsy throughout their life. Localization of the epileptogenic region during pre-surgical planning is far from perfect and may lead to partial or complete resection of certain brain regions responsible for cognitive skills, memory processes, etc. Thus, there is a need for an alternative method to treat epilepsy for a better quality of life. Robust seizure prediction may be considered as a future option, but it is still in a research stage.

While some patients experience auras, which are perception or feeling perturbations that act as warning symptoms of an imminent seizure, attempts at algorithmic seizure prediction have been considered only since the 1970's. Many past research efforts have been conducted with an aim to identify precursors of seizures, but actual reliable indicators are still unknown. Early attempts for seizure prediction were made using preictal spikes. It was seen that spikes possibly inhibit seizures or decreased rate of spikes indicated the secondary symptoms of seizures and spikes before seizure are patient specific (Karoly et al.,2016). But in recent studies, high frequency

oscillations (HFOs) are emerging as promising biomarkers of the seizure onset zone in epilepsy (Jacobs et al., 2009; Zijlmans et al., 2012), but it is still unknown whether HFOs are seizure precursors, the cause of seizures, or generated as a result of seizures.

1.1 Problem Statement

In this study we aim at assessing the rate of interictal high frequency oscillations (HFOs) associated with the seizure onset zone and we aim to validate and compare automatic HFO detectors. Studies show that HFOs are locally generated and can be seen in both physiological and pathological processes of the brain. Due to incomplete knowledge of morphology of HFOs in time signals, i.e., amplitude variations, time duration of their occurrence, etc., it is hard to distinguish physiological HFOs from pathological ones. Some studies define gamma signals (80-150Hz) and ripples (150-250Hz) as related to physiological processes while associating fast ripples (>250Hz) with pathological activity (Zelmann R. et al., 2009). Also, co-occurrence of ripples and fast ripples is associated with pathological signals (Sarnthein J. et al., 2017). While others refer to the entire 80-500Hz range (with an upper limit based on sampling rate) as pathological (Zijlmans et al 2012). Thus, due to this dilemma, in this research, we hypothesize that any HFO seen near the seizure onset zone (SOZ) in an epileptic brain is pathological.

There are many algorithms used for the detection of HFOs in electroencephalographic (EEG) signals. These detectors are verified in their sensitivity and specificity with respect to visual marking of HFO events by an expert. As it is to be expected, there is no consistency of marking criteria across experts. In previous research work, we can see two or three verifiers (Zelman R et al 2012) participating in event marking to establish the ground truth, but not all events are marked by all reviewers. Some events are marked as either false or true by different experts. In addition, visual marking is a time-consuming process. Through this research we found also this type of

differences amongst the detectors, i.e., each detector had events apart from those commonly accepted by the utilized detectors. One assumption made when using automatic detectors is that different detectors will agree on detected HFOs in a given signal. Most of the researchers aim at comparing the HFO rates with respect to visual markings by experts. However, events not recognized by the visual marker may be identified by an automatic detector and may be rejected as a false event since it does not coincide with the visual marking. Thus, in this work we are comparing the time of occurrence of events according to detectors and verifying their sensitivity and specificity based on our HFO definition as the ground truth. We propose using the combined results of HFO events seen by detectors for seizure prediction.

Even though existing research claims work on automatic detectors, they are not completely automatic. In addition to having to set thresholds and other parameters for HFO detection in a given data set, they still require visual validation by experts to accept or reject detected candidate events. As an extension of our initially planned work, in this research an attempt is made to classify candidate events applying machine learning techniques to event spectrogram images.

1.2 Related Works

Seizure prediction is a research area that has been active for several decades, the brief literature review below will provide some necessary background. The first paper provides an insight about how HFOs are seen in physiological processes (Kucewicz M.T. et al., 2014), the second paper covers surgical outcomes on HFO-generating areas (Fedele, T. et al., 2017), the following paper discusses HFO visibility on scalp electrodes (Zelmann et al., 2014), finally, a comparison of some detectors that are used for automatic detection of HFOs is presented (Zelmann

et al., 2012). In addition, the M.S. thesis of a student from the University of Texas El Paso (Kern, B.D. et al., 2016), which was chosen as the basis for our work, is discussed.

High frequency oscillations are associated with cognitive processing in human recognition memory (Kucewicz M.T. et al., 2014).

HFOs are associated with physiological processes like cognition and pathological processes like seizures. Ripples (120-250Hz) are known to be associated with memory consolidation, planning and decision making; fast ripples, even though mostly associated with epileptogenicity, can also be seen in normal physiological processes (re cited). This paper analyzes the association of HFOs with task-based memory processing, which includes encoding and recall processes. To analyze the encoding process, a set of 80 images from the International Affective Picture Set were presented to patients. Each image was displayed for 6s followed by 2s of blank screen. They were asked to rate images by pressing labeled keys on the scale of 5 ranging from 'very unpleasant' to 'very pleasant' with an interval of 6s preceding the next trial. Further, recall tasks used 140 images including previously presented images. The patients were supposed to identify the image to be 'new' or 'old' and the certainty of their decision was asked to be ranked on a scale of 3. Data obtained with this process was from intracranial recordings. Both with the encoding and recall tasks, HFOs followed a sequence coinciding with a theoretical model of the ventral visual stream (Mishkin et al. 1983 cited in Michael, T. et al., 20XX). Visual processing and encoding followed the following paths: occipital cortex (after image presentation), para-hippocampal, hippocampus, amygdala, and temporal and pre-frontal cortex. The paper reported a higher rate of induced HFOs (as a result of task-based function) during the recall process than during the encoding process. Also, it reports to have seen all bands of HFOs (80-500Hz) and more in the temporal and frontal lobes, which are known for memory processing. However, in this

research, HFOs are seen in terms of frequency ranges. Thus, the morphological differences between physiological and pathological HFOs still remain a question. Even though the patients involved in these tasks were diagnosed with epilepsy, the paper fails to report the consequences of the tasks on patients, i.e., whether the induced HFOs in turn induce any clinical or subclinical seizures in the patient.

Resection of high frequency oscillations predicts seizure outcome in the individual patient (Fedele, T. et al., 2017).

The viability of HFOs in seizure prediction can be determined only through surgical outcomes when HFOs are considered for surgical planning. This research correlates resection of tissues producing HFOs with seizure-free surgical outcomes. This paper defines a new region in the epileptogenic zone (EZ) apart from the seizure onset zone (SOZ) referred to as the HFO area. The HFO area is an EZ region with electrode contacts exceeding 95% percentile of co-occurrence of ripples (80-250Hz) and fast ripples (250-500Hz). EEG patterns consisting of at least 4 contiguous oscillations in the frequency range of 80-500Hz that clearly stand out from the background are considered as HFOs (Zelmann, R. et al., 2012). This paper reports seizure freedom in 13 patients out of 20 whose resection involved complete resection of the HFO area. Six out of the 13 above had an SOZ that extended to other regions of their cortex. The remaining 7 patients are reported to have recurrent seizure as the surgical outcome due to limited coverage of implanted electrodes. Of the above seven patients, one had resection of the complete frontal cortex. Even though this paper gives a good sense of the relation between the HFO area and seizure freedom, this result needs to be verified in a large number of patients. More analyses need to be done to verify whether the HFO area is better than the SOZ to delimit the resection area.

Scalp EEG is not a Blur: It Can See High Frequency Oscillations Although Their Generators are Small (Zelmann, R. et al., 2014).

This is a research paper about visibility of high frequency oscillation in non-invasive recordings. Due to the small amplitude of HFOs and the resistivity of the skull, it was previously assumed that the HFOs were visible only with invasive methods using subdural grids. In this paper, simultaneous scalp and intracranial recordings are used to verify the visibility of HFOs in scalp electrodes. Through this work, Zelmann, R. et al., 2013, showed that HFOs can be indeed seen in scalp electrodes – even though a few are missed, as the sizes of regions of cortical HFO generators are small. Another reason for this problem is that scalp and intracranial electrode configurations are spatially undersampling the brain. Even intracranial electrodes miss a few HFOs if they are not directly placed on HFO generators. Their working HFO definition is "HFOs are events with at least four oscillations of sinusoidal-like morphology in the filtered EEG that stand out from the surrounding background (Worrell et al 2012)." This research does not say how skull conductivity, other tissues, and muscles affect the amplitude of HFOs visible on the scalp. A right set of electrode configuration for intracranial and scalp EEGs to recognize all the HFO activity is yet to be found.

A comparison between detectors of high frequency oscillations (Zelmann, et al., 2012)

Visual marking of HFOs by experts gives a clear understanding of HFOs relation with epilepsy, but this method for detecting events is highly time consuming. Thus, there is a need for automatic methods to identify HFO events. In this research, a few detectors are compared to determine their detection reliability. The detectors used are the short term energy method (STE), the short line length method (SLL), a method based on the Hilbert transform (HIL), and the

Montreal Neurological Institute method (MNI). These methods were later included in the Matlab based open source software called RippleLab. For comparison purposes, the definition of HFOs used here is "EEG patterns in the range of 80-500Hz, consisting of at least four oscillations that can be clearly distinguished from the background." The detectors are compared using sensitivity and specificity of the detector with respect to visual recognition of events in the signals.

The first method discussed is the short-term energy detector (STE), which is also referred to as the RMS detector. This detector was developed by Staba et al., 2002. Each channel is first filtered using a band pass filter at 80-500Hz. Then using a 3-ms sliding window, energy is calculated as the root mean square (RMS) of the amplitude. The standard deviation is used for a threshold to distinguish the HFOs from the background. Segments with 5 times the standard deviation of the mean energy of the whole EEG with more than 6ms of duration (<667Hz) were considered as HFOs. With default settings, this method has less sensitivity compared to other detectors. While several HFOs were disregarded, the true events were more than the false events.

The second detector is the short line length detector (SLL), also referred to as the Line Length detector. This method was developed by Gardner et al., 2007, and has been applied on microelectrode and macroelectrode montages, but with macroelectrodes, no fast ripples were detected. First, the signal is passed through a first order differential filter to equalize the spectrum. Then each channel is band passed between 90Hz-1kHz. Energy threshold is computed as the 95^{th} percentile of the empirical cumulative distribution function of 3-min epochs. This method is reported to have the lowest sensitivity compared to other detectors and the highest false detection rate.

The third detector uses the Hilbert transform to compute the envelope of the signal. This is a method developed by Crepon et al., 2010. Each channel is filtered first with a 180-400Hz bandpass filter. Events with 5 times the standard deviation of the envelope over the whole EEG are considered HFOs. This detector is reported with the lowest sensitivity compared to other detectors and a high false detection rate. This detector was developed with a different HFO definition and this may be is a reason for the detector's poor performance.

The final method is the Montreal Neurological Institute detector (MNI). This detector consists of two methods – one with baseline detection and the other without baseline HFO detection. Each channel is band-passed between 80-450 Hz forward and backwards to achieve zero phase. Then, to determine which method to use, baseline detection is performed. A segment is considered to be baseline if it does not contain any kind of high-frequency oscillatory activity. For baseline detection, wavelet entropy is used on the autocorrelated signal to measure the degree of randomness or content of oscillatory activities in the signal. The EEG is then divided into segments of 125-ms. Next, the normalized wavelet power is computed for autocorrelated segments and the maximum theoretical entropy is calculated where the signal resembles white noise. Thus, a baseline is considered if the wavelet entropy is larger than the threshold obtained through training.

If a baseline is found using the method above, in order to perform HFO detection, the signal RMS value is calculated using a sliding window like the RMS detector. HFOs are distinguished from the background using the threshold calculated as the empirical CDF value of the baseline segment, as opposed to using the entire signal. A CDF within the 99.9999 percentile is chosen as the threshold. If there is not enough baseline detected, the RMS value is calculated in one-minute segments for each channel using a sliding window. Due to the absence of a baseline, the threshold value is at the 95 percentile of the CDF of the segment. On the one hand, in comparison to the

other methods, the MNI method had better performance in terms of detecting a higher number of events. On the other hand, even though this method detects more events, it has the highest false detection rate.

One thing to note is that all the above-mentioned detectors were developed with different datasets and HFO definitions. However, since only the number of detected events is important here, the MNI methods outperforms other detectors in this research with at least 80% of HFOs detected. Since the detectors were used here with the default values for their dataset, the same default may not be applicable to all datasets, i.e., the parameters may be patient-specific. Even though these detectors reveal potential HFOs in EEG signals, the final decision as to whether detected events are HFOs is made by the visual acceptance or rejection of an expert.

The viability of high frequency oscillation analysis in EEG signals for seizure prediction (Kern B.D. et al., 2016).

This is a master's thesis of a student from University of Texas at El Paso. This research aims to verify whether the rate of HFOs in the seizure onset zone (SOZ) during the preictal period changes with respect to the rate of SOZ HFOs during the interictal period to enable seizure prediction. This work is on a single patient data and with a minimal of patient specific and electrode placement details. It uses raw EEG signals from the Epilepsiae database with a 2500Hz sampling frequency. First, intracranial EEG data was high-pass filtered at 0.5 Hz to remove the DC bias. To determine the SOZ, signals were filtered with a low-pass filter at 70Hz. To use an energy threshold method, the energy of the signals is computed as E(t) = $\sum_{k=t-n+1}^{t} x^2(k)$. The channels with energy crossing the threshold defined as 3 times the standard deviation of the signal were ranked. The first five channels crossing this threshold were chosen for HFO detection. Selected channels

were then low-pass filtered at 625Hz and processed with RippleLab (Navarrete et al 2016). Keeping the threshold for detection without a baseline constant at the 95 percentile, the threshold for detection with a baseline was changed in order to obtain a greater number of HFO candidate events. This was repeated on the last 20 minutes of the preictal period of all 9 seizures the patient had. The interictal period chosen was a 20-minute segment in a twelve-hour seizure-free period. This work reports finding a 20-fold increase of HFO rates in the preictal period compared to interictal period rates. However, this needs to be verified with a greater number of datasets from more patients in order to conclusively determine whether preictal HFO rate increases are robust indicators of imminent seizures, i.e., to determine whether, in general, preictal HFO rates are monotonic functions or step function for all seizure instances.

Chapter 2

Theoretical Foundation

This chapter consists of topics that are used as background for our work. Here we discuss the frequencies of electrical brainwaves, the electroencephalogram – which is used for measuring electrical activity of the brain, the seizure onset zone – which is considered as the region of the brain where seizures originate, a brief description of signal energy used in our work, and probability distributions considered for thresholds in our work.

2.1 Frequency bands involved in electrical brain activity.

Brain waves or neural oscillations are a synchronized electrical pulse produced by ionic or electrical conduction during neuronal communication. These waves are measured using electroencephalograms (EEG). EEGs can be recorded from the scalp or through invasive methods. Brain waves are characterized based on their frequency range as clinical frequencies that are associated with normal brain activity or HFOs associated with seizures.

Clinical EEG frequency see Figure 2.1, ranges from 1-70Hz and it is further characterized as infraslow (<0.5Hz), delta (0.5-3Hz), theta (3-8Hz), alpha (8-12Hz), beta (12-38Hz), lower gamma (38-70Hz) as shown Figure 2.1. Infraslow signals are cortical signals associated with brain timing and network functions. Due to their slow nature and traditional filtering, it is difficult to detect them. Delta signals (0.5-3Hz), also known as deep sleep waves, are generated during slow wave sleep and during meditation. This triggers secretion of growth hormone indeed providing a healing effect. Theta signals (3-8Hz) are observed in the REM sleep stage. They are associated with dreams, imagination, intuition, and learning processes. They are also seen during fear stressed emotions. Alpha signals (8-12Hz) are associated with the rest state of mind. They can be observed

when a person is calm and relaxed, during mental coordination, and alertness. Beta signals (12-38Hz) are observed in the conscious state or waking state of a person. They are associated with focus, problem solving and decision-making skills. Lower gamma signals (38-70Hz) are associated with simultaneous information processing in different brain regions and a high attention state (Tatum et al., 2014).

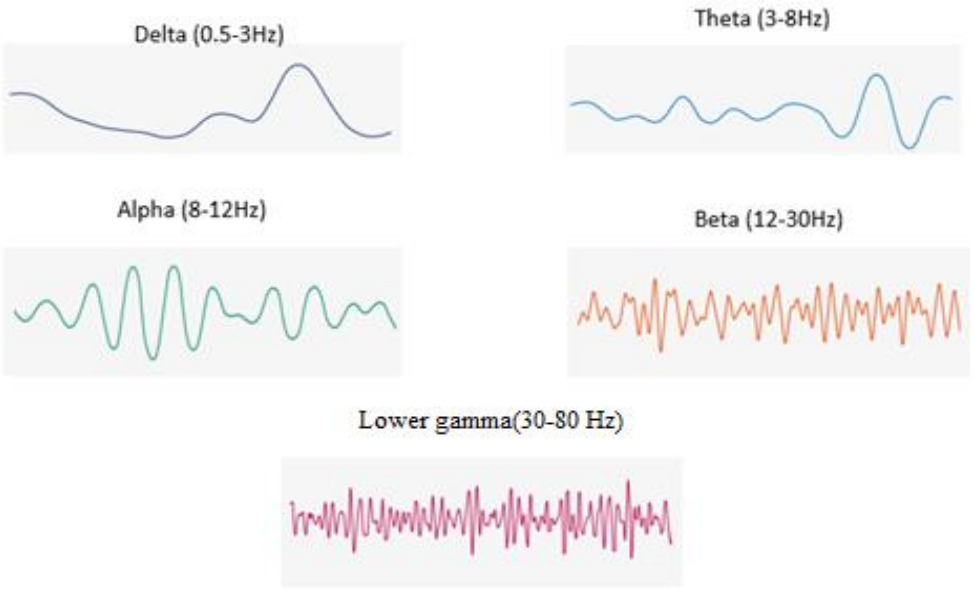

Figure 2.1 Traditional EEG frequency ranges used for clinical practice.

Visible HFOs range from 80Hz to over 500Hz based on the sampling rate of the signals during recording. HFOs are characterized as either upper gamma (80-150Hz), ripples (150-250Hz), or fast ripples (> 250Hz). Studies indicate that HFOs are associated with seizures and have been identified as biomarkers of seizure generating tissues. With recent studies, HFOs have been determined as locally generated cortical signals associated with the seizure onset zone (SOZ) and seizures. HFOs are described in distinct approaches based on researchers' points of view. Some descriptions include signals in the 80-500Hz frequency range (Roehri N. et al., 2018, Zelmann R. et al., 2009), spontaneous EEG patterns consisting of at least 4 oscillations of frequency 80-500Hz that can be clearly distinguished from background with time duration of at

least 25ms (Zelmann R., et al. 2012, Sarnthein J et al., 2017), events with 3 consecutive cycles with amplitude higher than the average of the background (Gotman J., et al. 2012), and an increase in a time-frequency (TF) graph that is wide enough in time but has limited spread in frequency (Roehri N et al. 2017). Thus, in this work HFOs are defined as signals with at least 4 oscillations in the frequency range 80-500Hz, with at least 25ms duration, and a TF representation which is wide enough in time and limited in frequency.

2.2 Electroencephalogram

Electroencephalography is an imaging technique to detect and record electrical activity from the brain as amplitude plots over time referred to as electroencephalograms (EEG). EEGs can be recorded in a non-invasive manner from the scalp with surface electrodes or invasively using grids of electrodes on the brain cortex (iEEG) or depth electrodes, as shown in Figure 2.2 Scalp EEGs are prone to have high levels of noise and loss of information due to muscle activity, skull conductivity, eye movements, and power line interference (Teplan, 2002). Several studies have proven that HFOs can be visible on the scalp (Zelmann R et al., 2014) but the visibility rate of HFO is less compared to iEEG. For this reason, in our study we focus on iEEG in order to have less noise and have a higher rate of HFOs in analyzed signals.

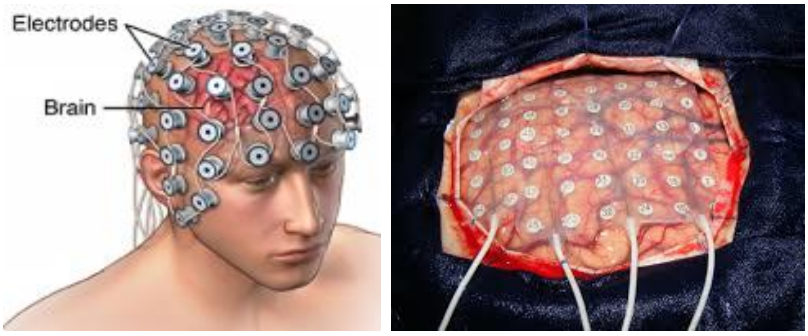

Figure 2.2 EEG recording methods.

A. Non-invasive EEG. B. Invasive EEG.

2.3 Seizure Onset Zone

The seizure onset zone (SOZ) is defined as the region in the brain cortex where seizures originate and from which they propagate. In an epileptic brain, the SOZ can be considered as a subspace of the epileptogenic region. As the exact location of SOZ is hard to determine during recording, we hypothesize that the electrode that sees the seizure first is the electrode that is directly placed or placed closer to SOZ. During surgeries, resection of the entire SOZ may not result in a successful surgical outcome. This may be because the SOZ may not represent the entire epileptogenic region or due to early seizure onset or early seizure spread. “HFOs are said to occur in regions where the threshold is low for cortical stimulation to give rise to after-discharges or evoked seizures, even outside the seizure onset zone” (Zijlmans M et al., 2012, Jacbobs J et al., 2010).

2.4 Root mean square value

The Root mean square (RMS) value describes the strength of a signal. It is given by the equation (Navarrete M et al 2016)

$$E(t) = \sqrt{\frac{1}{N} \sum_{k=t-N+1}^{t} x^2(k)}$$, N = window size

The software tool used for our research, RippleLab, uses RMS values as the basis for detecting HFOs. In a normally distributed signal, the RMS value is equal to its standard deviation.

2.5 Probability Distribution

In statistics, probability distribution is a mathematical function used to understand the characteristics of random data. Some of the parameters commonly used in probability distribution analysis are mean – an average of all the data values, standard deviation – dispersion of data about the mean, probability density function – the relative probability that a variable will take the value of a given sample, cumulative distribution function – probability of a variable to take a value less than or equal to a given sample. The most commonly used continuous probability distribution is the Gaussian or normal distribution, but there are many more distributions like gamma, beta, etc.

The normal distribution is a continuous probability distribution represented by a bell-shaped curve in which the data is distributed symmetrically about the mean value. Whenever we have an unknown sample of an experiment, the first assumption about the sample set is that it is distributed normally. The function is given by the following equation(Kay et al 2006).

$$f(x) = \frac{1}{\sqrt{2\pi\sigma^2}} \exp(-\frac{(x-\mu)^2}{2\sigma^2})$$

where μ is the mean or expectation, σ is the standard deviation, and σ^2 is the variance of the distribution. In our work, the STE detector considers the signal to be distributed normally and its standard deviation is used as the HFO detection threshold.

The gamma distribution, the maximum entropy probability distribution, is also a continuous probability distribution, similar to the normal distribution, but its shape is not symmetric and it is a non-negative distribution. Its equation is given by (Kay et al 2006),

$$f(x) = \begin{cases} \dfrac{\lambda^{\alpha}}{\Gamma(\alpha)} x^{\alpha-1} \exp(-\lambda x) & x \geq 0 \\ 0 & x < 0 \end{cases}$$

where $\Gamma(\alpha)$ is the gamma function, α is a shape parameter, and λ is a scale parameter

In our work, the MNI detector considers EEG signals to be distributed as a gamma distribution. Due to non-symmetry of the distribution, the standard deviation of the distribution is zero. Thus, the MNI detector computes an empirical cumulative distribution and a certain percentile, which is patient-specific, is used as a detection threshold. Every detection analysis uses different statistical assumptions tailored around analyzed data. To date, there is no common set of statistical assumptions that gives a generalized idea about EEG signals.

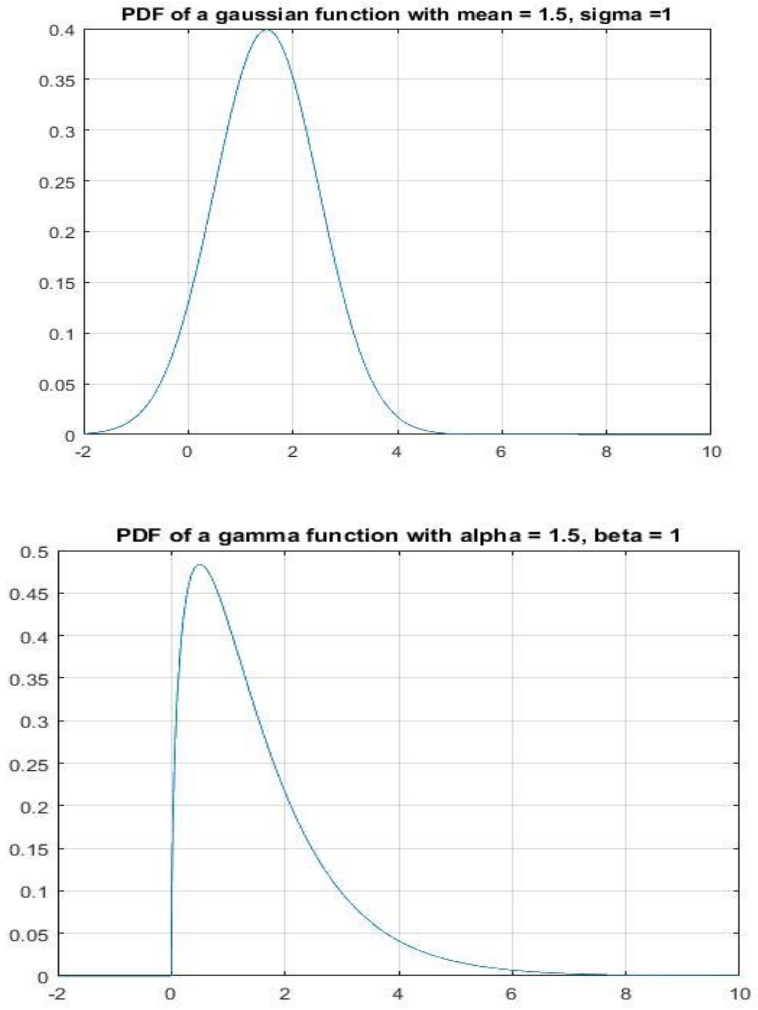

Figure 2.3 Gaussian and gamma probability density functions.

Chapter 3

Software tools

Researchers use different software and techniques for HFO detection. Below are some of the tools used for our work. We begin with filter design techniques followed by Epilab, a tool used for visualizing EEG signals. Then we discuss RippleLab, the HFO detection tool that we used. Finally, we discuss Alexnet, a deep learning toolbox we used to explore the performance of a deep learning approach to classify detected HFO events.

3.1 Digital Filtering with Matlab

In signal processing, we use filters to enhance features in sampled signals. Digital filters are used for discrete signals. Design of digital filters is subjected to the feature of interest. For this research, filters used for preprocessing of the signals were designed in a Matlab user interface tool called the filter design and analysis (fda) tool, one such low-pass filter is shown in Figure 3.1. This tool allows the user to visualize the magnitude and phase response of a filter, stability with pole-zero plots for infinite impulse response (IIR) filters, and group delay to check the delay that the filter might introduce in the signal. Further, ‘filter’ and other in-built functions were used to filter the signal based on the choice of filters (Proakis et al., 2001).

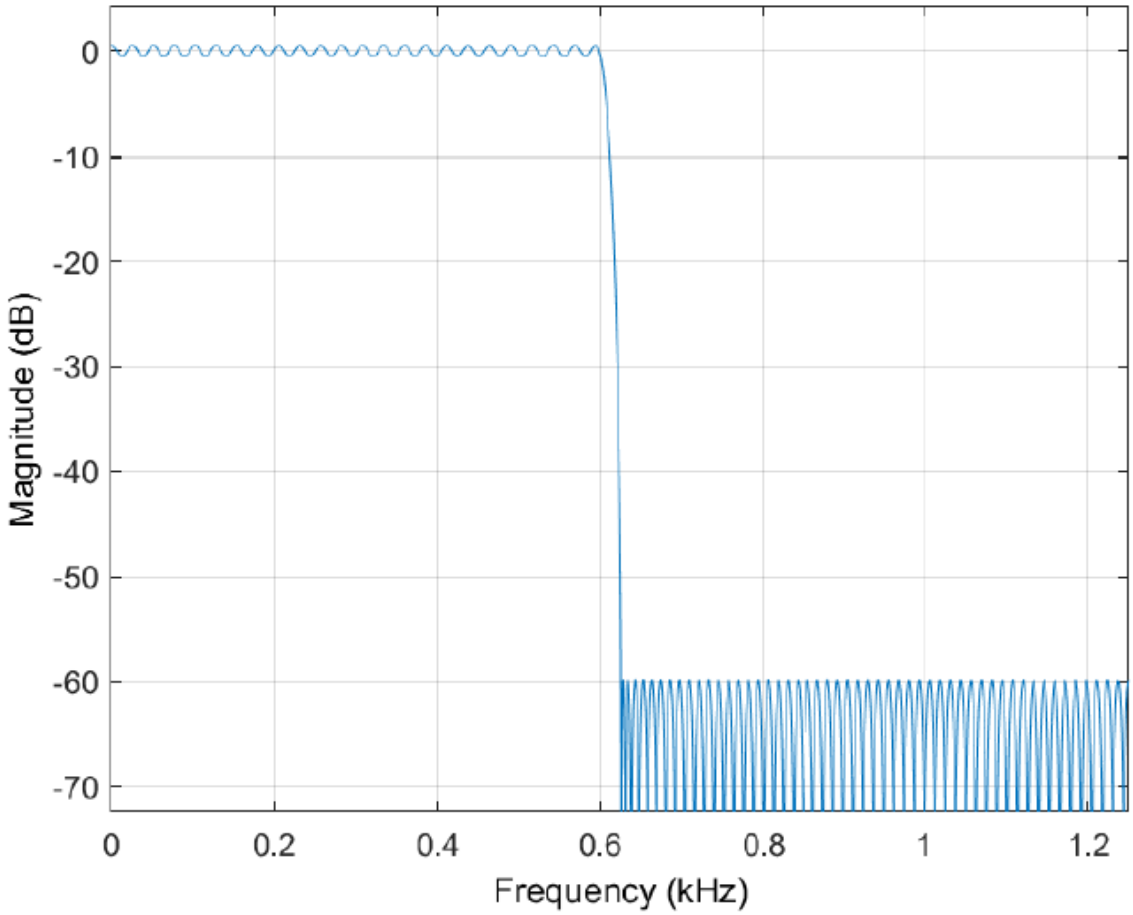

Figure 3.1 Magnitude response of FIR low-pass filter designed using fdatool resulting in filter order N=198.

3.2 EPILAB for EEG data handling

For visual verification of seizures in the signals, we used a Matlab based software package called EPILAB and developed as a product of the European project Epilepsiae. It is a graphical user interface developed for statistical validation of signals for seizure prediction (Teixeria et al., 2011). It uses high dimensional feature space, threshold and classification methods for seizure prediction. A general overview of the tool is shown in Figure 3.2. Since we are interested in HFOs and their features are still a question, we used this tool for visualization of EEG signals as seen in Figure 3.3 and verification of seizure onset and offset time provided in the database.

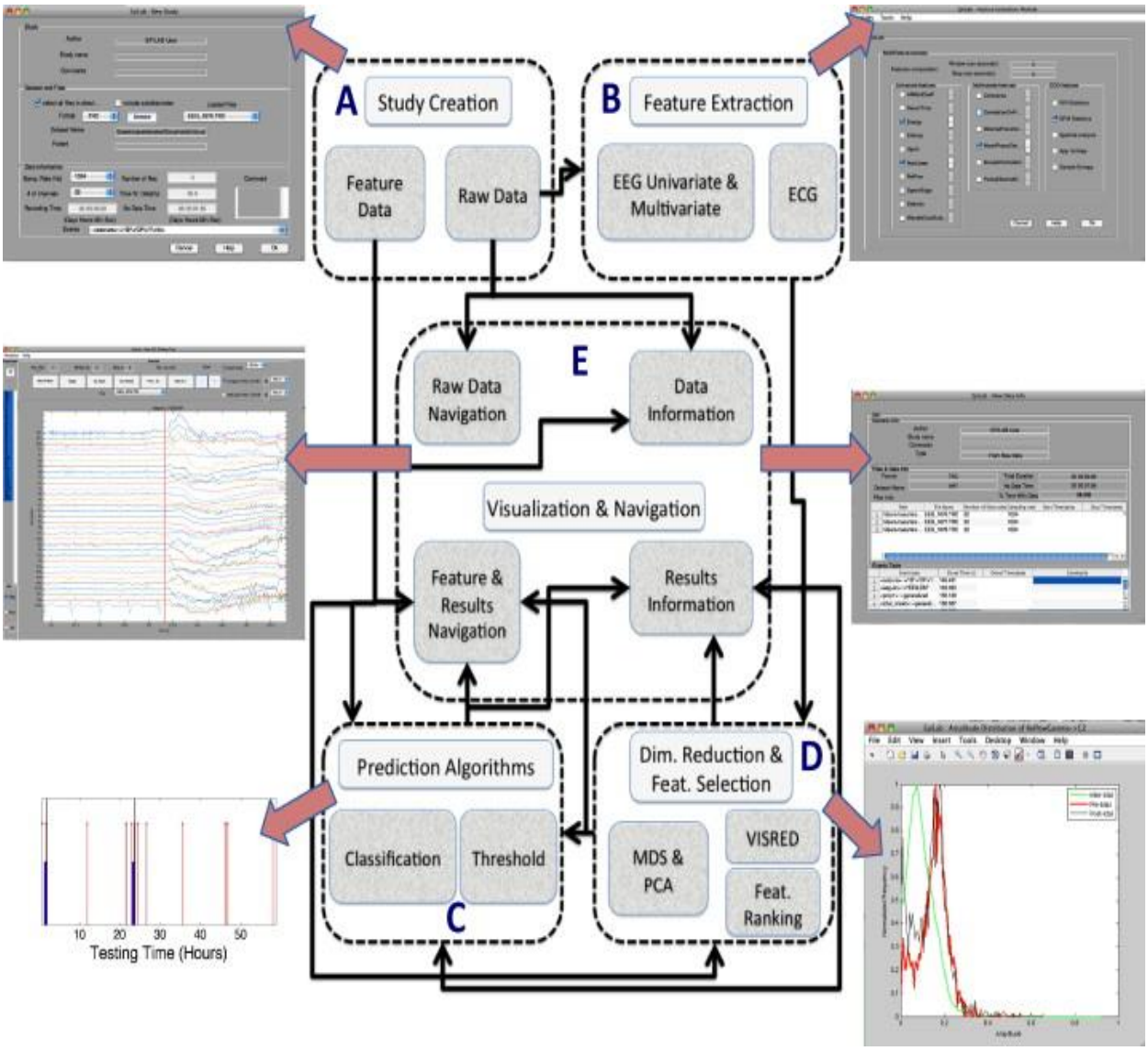

Figure 3.2 Epilab user interface from Teixeria et al., (2011).

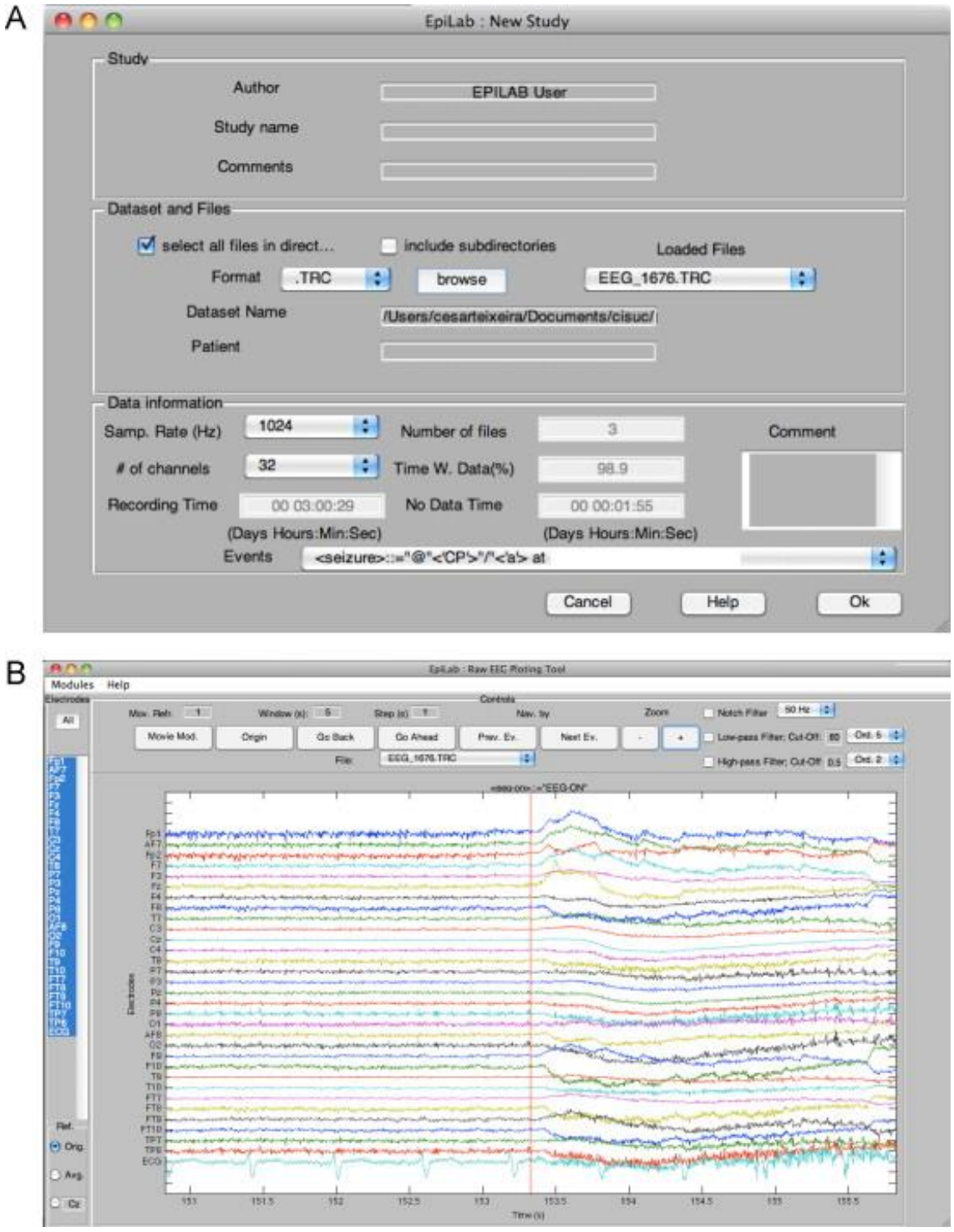

Figure 3.3. Epilab study creation and data navigation from Teixeria et al., (2011).

3.3 RippleLab for HFO Detection

There are several open source computational tools that are been proposed by several research groups (Navarrete et al., 2016), but there is no HFO detection algorithm that works best under all conditions. Every detector algorithm is developed based on certain human or animal data, but it is never compared to other detectors with other sets of data and descriptions lack the adequate settings for manual or automatic detection and validation of the events. Thus, in order to overcome this problem, a research group from Colombia developed a MATLAB open source application called RippleLab. It has a graphical user interface (GUI) for identification, selection, and validation of candidate events as shown in Figure 3.4 .

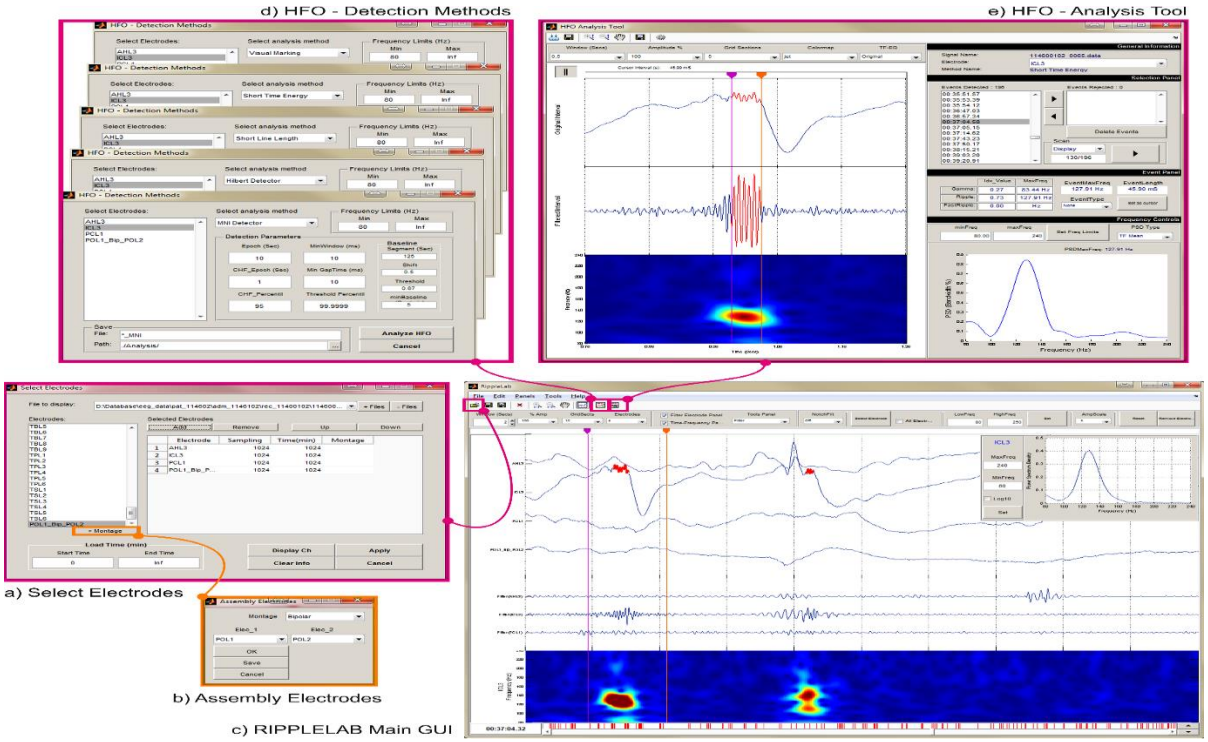

Figure 3.4. RippleLab interface from Navarrete et al., (2016).

RippleLab incorporates four HFO detection algorithms as discussed in Chapter 1. Out of the four detectors in RippleLab, we decided to work with the Montreal Neurological Institute (MNI) and short-term energy (STE) methods as both use RMS values to detect the events. For a sense of HFO detection using the MNI and STE methods we give an analysis of the algorithm of both the detectors.

The MNI detector uses baseline detection, energy computation, and thresholding methods to detect the candidate HFO events. For baseline detection, first the signal is band-pass filtered and then wavelet entropy is applied. For this, the signal is segmented, and its autocorrelation function is computed using the complex Morlet wavelet (Navarrete et al 2016). The baseline is considered if the minimum entropy is larger than a threshold. If there exists enough baseline, HFOs are detected with moving average energy (RMS value), as defined in Chapter 2, on the filtered signal using an empirical CDF as threshold for detection. The CDF value is defined by the user depending on the data. A flowchart of the MNI detector implemented in RippleLab is shown in Figure 3.5.

STE uses energy computation and thresholding methods to detect candidate HFO events. Energy is computed using the moving average (RMS value) as defined in Chapter 2. With three times the standard deviation and at least six peaks (user defined value) as the threshold, candidate HFO events are detected (Navarrete et al 2016). . A flowchart of the STE detector implemented in RippleLab is shown in Figure 3.6.

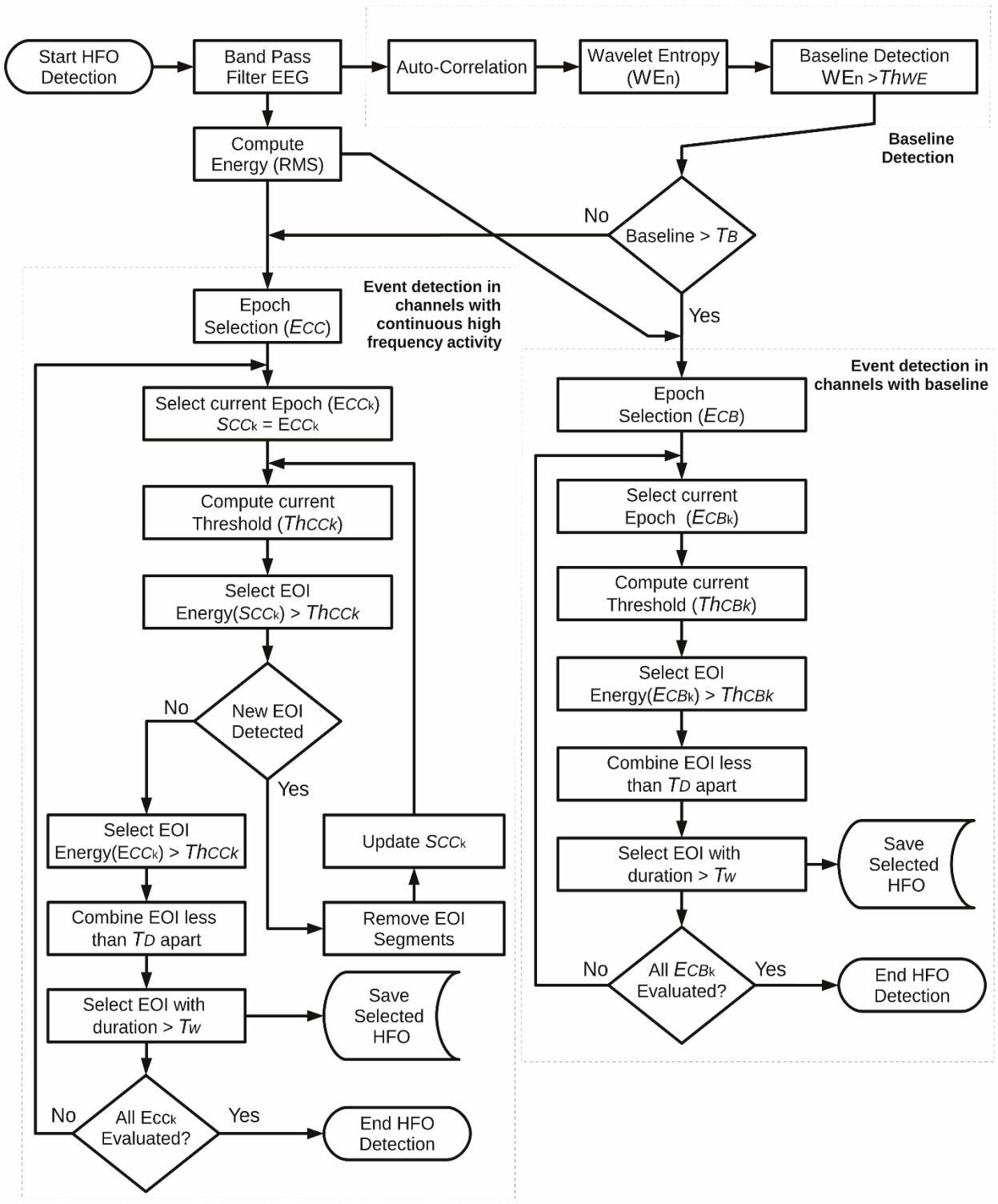

Figure 3.5. Flowchart of MNI Detector taken from Navarrette et al.,(2016)

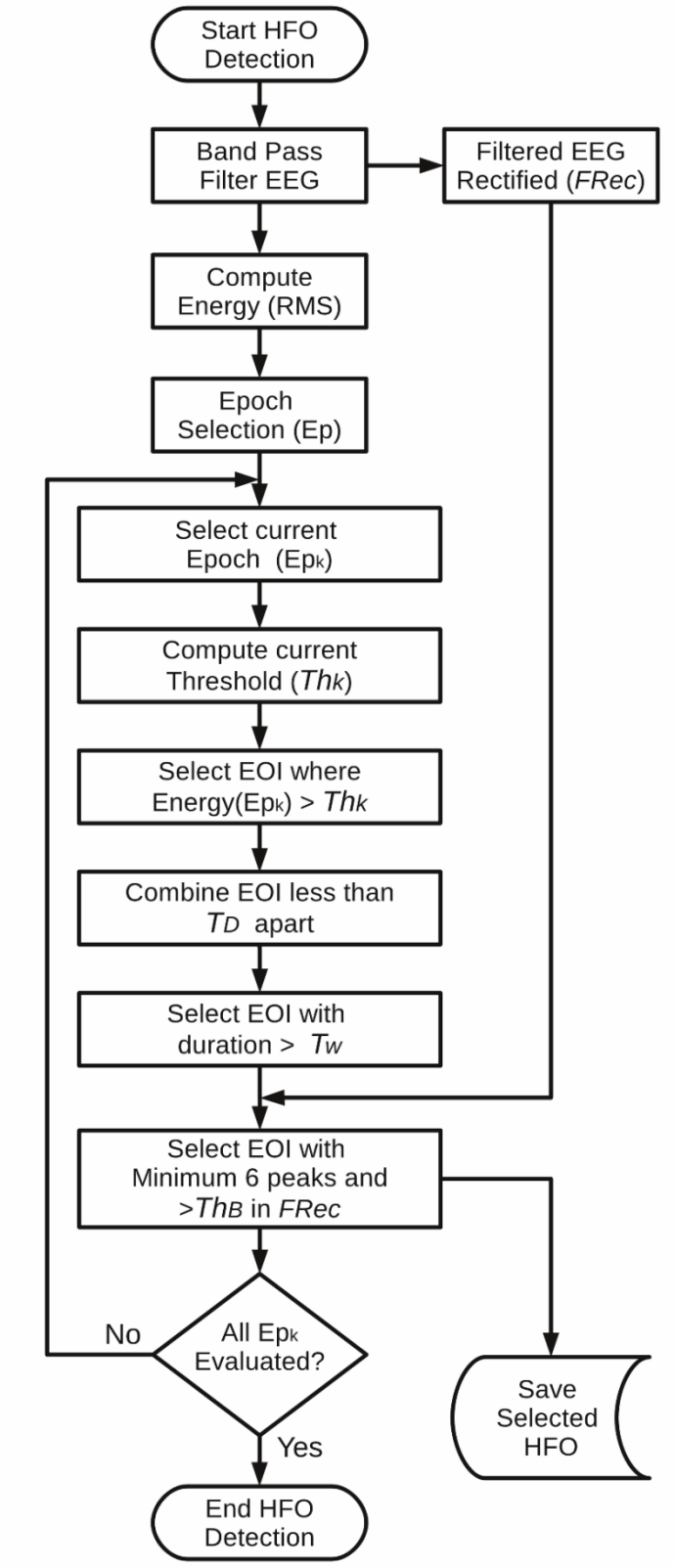

Figure 3.6. Flowchart of the STE detector taken from Navarrete et al.(2016).

3.4 Alexnet deep neural network

Artificial neural networks (ANNs) are a subset of machine learning methods inspired by mechanisms of interconnected neurons in a brain. Virtually all ANNs are comprised of large connections of input layers followed by hidden layers and output layers which contain neurons and weights that determine the outcome of learning. For an ANN to effectively learn something, a collection of data is required to train the network. There are several types of neural networks whose functionality and architectures differ depending on the application of the training and learning. The measuring techniques we use today to acquire brain data such as functional magnetic resonance imaging (fMRIs), electroencephalography (EEGs), etc. are lacking in information due to having either diverse temporal or spatial characteristics. An fMRI could provide good spatial resolution since it measures neural activity by measuring changes in cerebral blood flow. A drawback is that it could measure 6-10s after the initial excitation of a neuron which leads to poor temporal resolution. The opposite problem arises with EEG, which achieves great temporal resolution but poor spatial resolution. Therefore, a method of handling multimodal data is desired to do predictive modeling and, for the purposes of this research, gain understanding about how to detect HFOs and other biomarkers of seizures and the brain's response to treatments. We aim to develop an algorithm which uses information in time, space, and orientation from dynamic activity data and static orientation data (Sengupta et al., 2018). For the initial phase of implementing neural networks for HFO detection, we decided to use Matlab's Alexnet algorithm since it offers a fast and easy way to train and fine tune a pretrained network. Alexnet was designed by Alex Krizhevsky, and published with Ilya Sutskever and Krizhevsky's Ph.D. advisor, Geoffrey Hinton.

Alexnet deep learning toolbox has flexibility and resources to start training our own network. Its deep neural network was pretrained on about 1.2 million images from the ImageNet

dataset and can perform 1000 different classifications. Alexnet consists of five convolutional layers with rectified linear unit (ReLU) activated neurons followed by max pooling layers, three fully connected layers, and a final 1000-way softmax. The architecture consists of 60 million parameters and 650,000 neurons as a whole. Dropout is used as a regularization method in order to reduce overfitting of the model.Each neuron has a probability of 0.5 for being dropped . Its parameters are learned using forward and backward propagation techniques (Krizhevsky., A., et al., 2012). There are different ways of repurposing previously trained networks which are: classification, feature extraction, and transfer learning. Classification involves using the pretrained network directly for classifying a new image. Feature extraction uses the layer activations as features and can be used to train a support vector machine (SVM) as an image classifier. Transfer learning takes an already trained network and uses its layers to fine-tune on a new dataset which saves us from creating a neural network architecture completely from scratch. For the purposes of this research we used feature extraction and transfer learning. The architecture of Alexnet is shown in Figure 3.7.

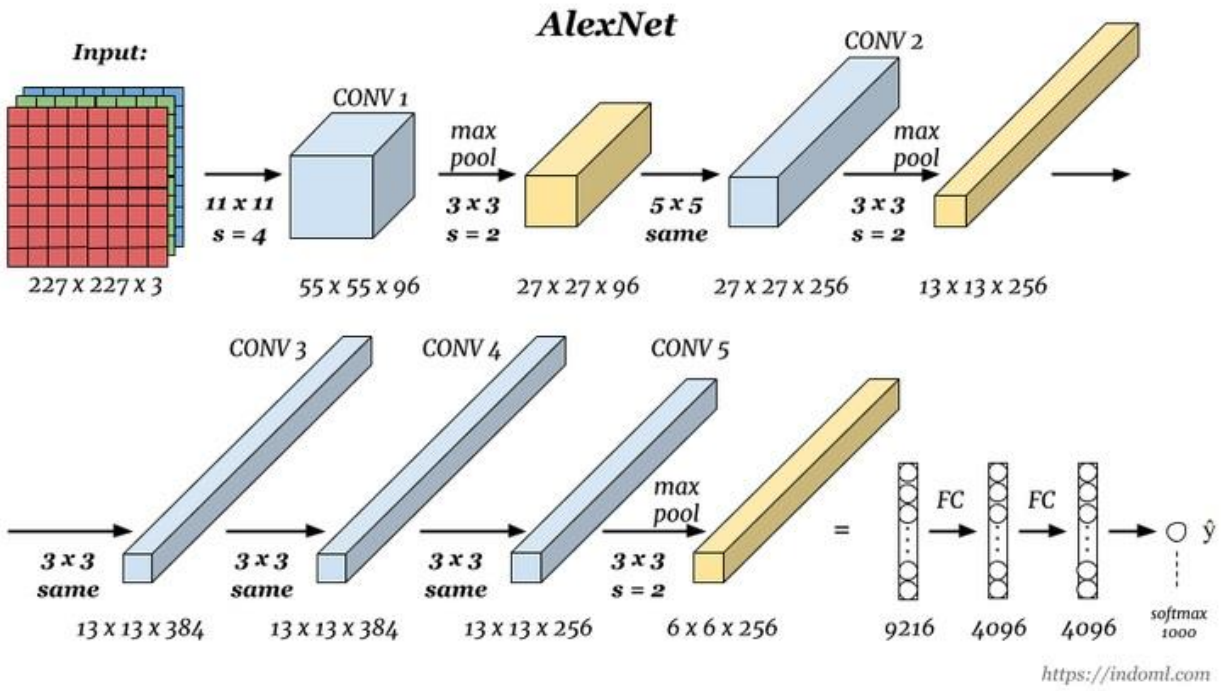

Figure 3.7. Alexnet architecture.

Chapter 4

Methodology

In this chapter, we discuss the EEG database and patient specific data that we used for our work followed by preprocessing of signals before preparing for HFO detection and analysis. Then, detectors and analysis methods used in our work are discussed. Lastly, we discuss event classification using the Alexnet deep learning toolbox.

4.1 The Epilepsiae Database

For our research, data from epileptic patients was accessed from the EPILEPSIAE database from Freiburg, Germany. The database consists of multiple epilepsy data sets, but most of them were sampled at 256Hz and unfit for HFO detection. However, we requested raw unfiltered data with a sampling rate of at least 2000Hz for this research. The data we received is from a single male patient of age 10. It was recorded over a course of about a week and it contains about 180 hours of continuous EEG. The data contains 62 twenty-minute intracranial recordings and 476 twenty-minute recordings acquired from intracranial and scalp electrodes. The intracranial recording is from an 8x8 grid and a 1x4 patch and the surface recording is from 20 scalp electrodes. The data also included EMG, ECG, and EOG recordings. The data was sampled at 2500Hz. The patient had 9 clinical seizures and 150 subclinical seizures as per the database. No ground truth for HFOs was provided within the signals.

Furthermore, we also obtained patient specific data from the database. The patient had undergone resection of frontal lobe tissue and callosotomy – a surgery of the corpus callosum to remove the connection between the brain hemispheres in order to prevent the spread of seizures in medically refractory patients. Even though the patient had localization specified as frontal lobe in the

database, the location of grids placed in the frontal lobe was not provided and MRI details were not made available for analyses.

4.2 Seizure Detection

Along with the patient surgical details, we also received details about the seizure origin electrode in the grid as shown in Table 4.1. The onset and offset time and sample of the seizures was provided by one of our contacts in Freiburg. To verify the seizures, we used the EpiLab tool introduced in Chapter 2. Since we did not have the required resolution to verify the onset time, we used the origins provided as the seizure onset zone (SOZ) and hypothesized that the patient suffered from generalized epilepsy. Thus, each seizure as has a different SOZ. Since we were not provided with post-surgical details and the patient has undergone callosotomy, the localization may not be identified correctly.

Table 4.1. Patient seizure data.

#	onset	Pattern	Vigilance	origin	Seizure Onset	Seizure Offset
1	eeg: 16.02.'11 11:31:04.683200	low amplitude fast activity(lafa)	unclear	GB6	639208	777630
2	eeg: 16.02.'11 14:33:48.943600	rhythmic beta waves	awake	GB5,GC4	2259859	2360140
3	eeg: 20.02.'11 23:18:08.978000	Polyspikes	Sleep stage II	FBA3,FBA4,GA6,GB5,GB6,GC4, GC5,GC6	1231878	1397677
4	eeg: 20.02.'11 23:18:08.978000	rhythmic beta waves	Sleep stage I	GA6	1584945	1748303
5	eeg: 21.02.'11 01:51:51.663600	rhythmic beta waves	Sleep stage II	GH1	799159	905620
6	eeg: 21.02.'11 02:58:25.760400	repetitive spiking	Sleep stage II	GF2	1784401	1903844
7	eeg: 21.02.'11 04:30:57.119200	repetitive spiking	Sleep stage II	GA5	662798	842632
8	eeg: 21.02.'11 08:28:39.692800	low amplitude fast activity (lafa)	Sleep stage II	GA6	319232	505437
9	eeg: 21.02.'11 22:51:59.313600	low amplitude fast activity (lafa)	Sleep stage II	GG3,GH3	818284	869052

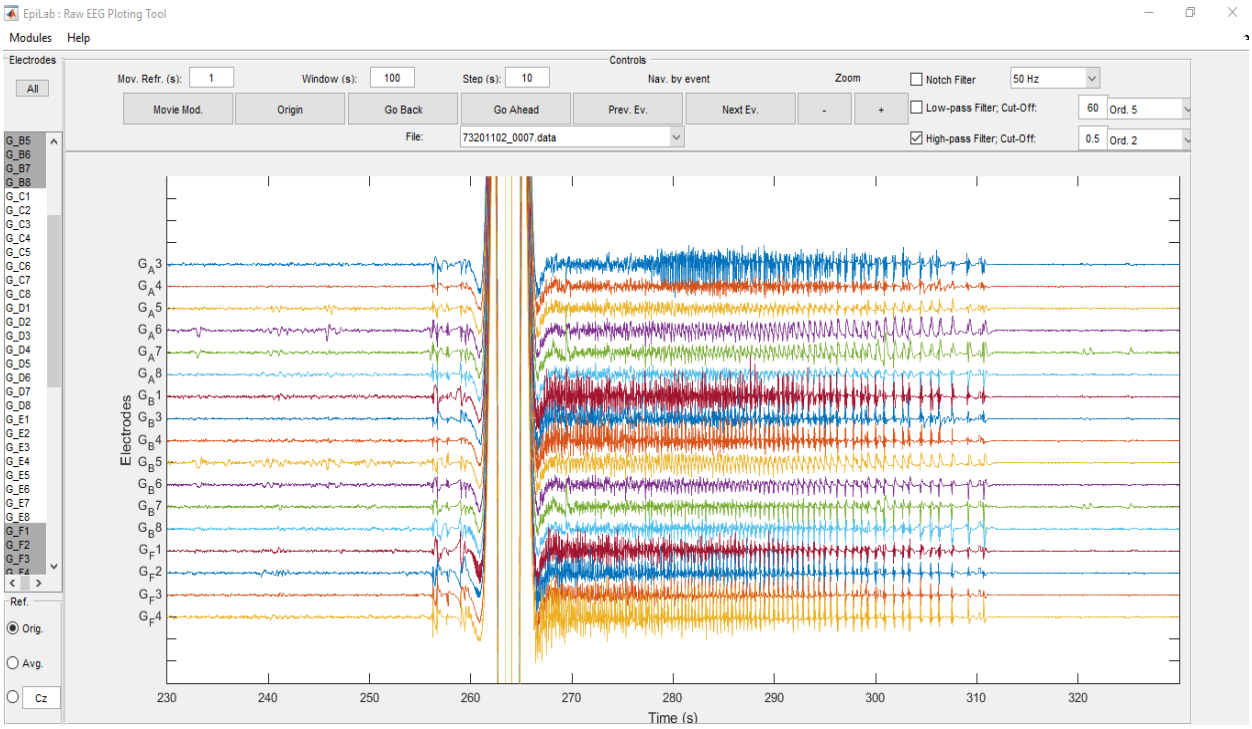

Figure 4.1. Epilab EEG data display.

4.3 Preprocessing of Signals

Filtering is the first step in EEG analysis, but there has yet to arise a standard approach for filtering EEGs, specifically with regards to HFO detection and analysis. Since there is no standard definition for HFOs and sampling rate that is required for HFO visibility (Zijlmans M et al., 2012), researchers develop filters based on their own HFO definitions. Early studies concentrated on frequency ranging from 30- 100Hz as HFOs. Later, oscillations only above 200Hz were considered as HFOs (Crepon et al., 2010). Most recent studies define HFOs as oscillations greater than 80Hz, which are further classified as gamma (80-150Hz), ripples(150-250Hz), or fast ripples(>250Hz) (Zijlmans M et al.,2012,Zelmann R et al., 2014).

For this research, we developed several filters for our experiments. Since the data used is raw and unprocessed, the first step was to remove signal bias, as shown in Figure 4.2, which is due to the EEG recording instrument. To accomplish this, we used an infinite impulse response (IIR) elliptical highpass filter (fStop = 0.05Hz; fPass = 0.5Hz; stop-band attenuation = -40dB; pass-band ripple=0.5dB, Fs = 2500Hz). Every signal was filtered with this filter as a preprocessing step. To prepare the signals for HFO detection and analysis, we used a finite impulse response (FIR) equiripple lowpass filter (fPass = 600Hz; fStop = 625Hz; stop-band attenuation = -60dB; pass-band ripple = 1dB, N=198) on every signal before downsampling it by a factor of 2. Furthermore, we used notch filters at 50Hz and its harmonics to remove power line noise.

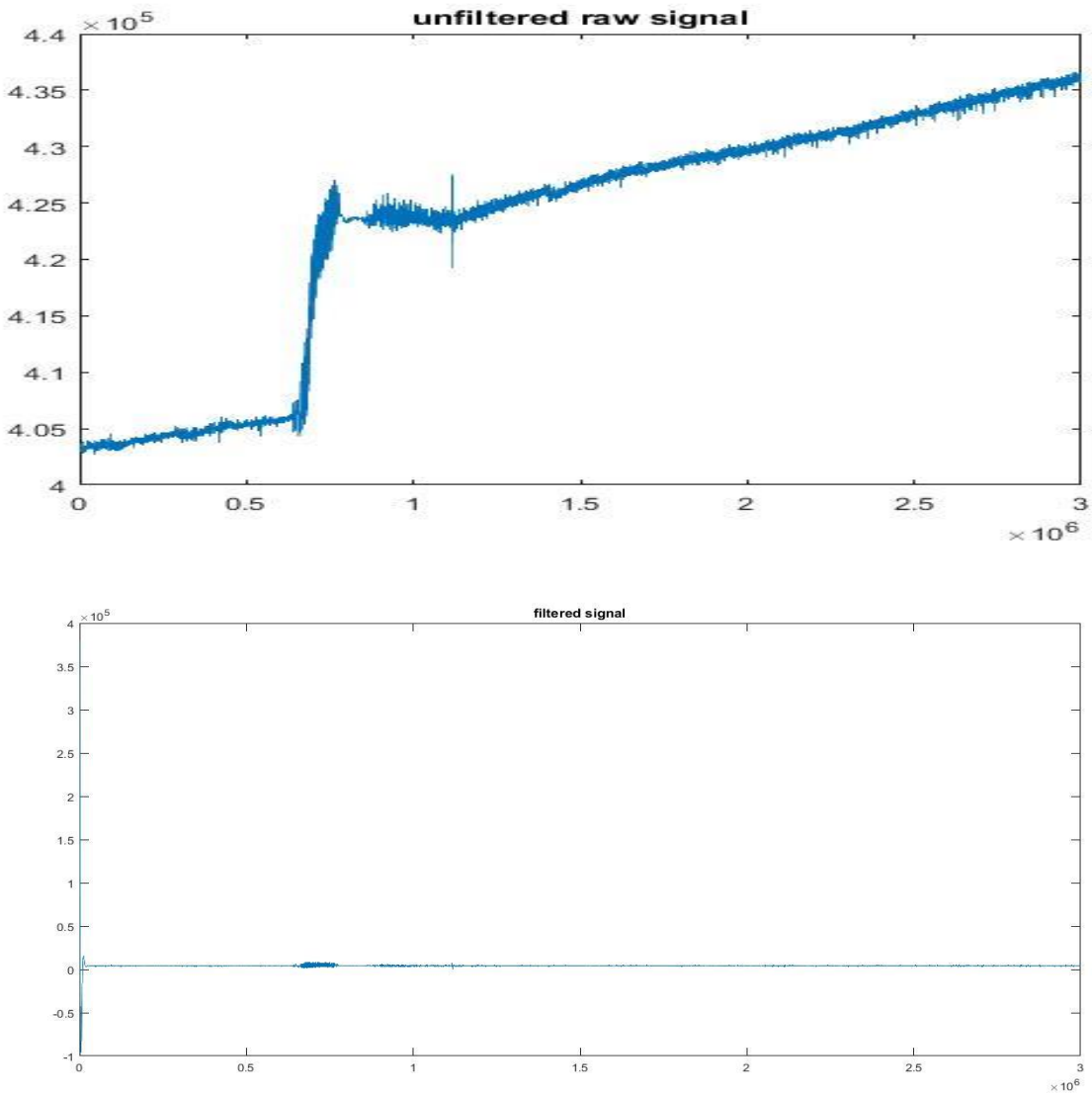

Figure 4.2. Unfiltered (top) and filtered signal (bottom).

4.4 HFO Detection

For HFO detection, we used the MNI and STE detectors included in RippleLab, which are discussed in Chapter 2. A brief outline of the detectors is discussed in Chapter 1. We noticed that parameters recommended in the paper by Zelmann, R. et al. (2012) are patient specific.

The MNI detector uses two thresholding methods for HFO detection. One for signals with a detected baseline and the other for signals without a baseline. Default settings for the threshold with a detected baseline is 99.9999% and for the threshold without a baseline is 95%. Recommended thresholds are 99% for signals with a baseline and 90% for those with no baseline. These parameters can be decided by the user. Previous research conducted in our lab by Kern, BD. et al. (2015) included 99.99%, 99.9%, and 99% while keeping the baseline threshold constant at 95%. In this research, we wanted to see for what value of thresholds we would get more HFO with less noise included. For this detector and our data, a 98% threshold with baseline of 95% worked the best with relatively lesser noise

The STE detector has a default setting of a 600s epoch time, a minimum of 6 peaks, an RMS window of 3s, and 5 times the standard deviation used as threshold for HFO detection. However, these parameters are subjected to signal length and HFO definition. For our research, we used a minimum of 4 oscillation and 600s epoch with remaining settings being the default value.

The threshold values chosen in both methods above are based on the consideration of statistical distribution of EEG signals. While the MNI detector considers signals to have a gamma distribution and uses the cumulative distribution of the signals for thresholding, the STE method considers signals to be normally distributed and uses its RMS value as a threshold. In normally

distributed signals, the RMS value as defined in chapter 2 is equal to the signal's standard deviation. These two detectors were used both on the preictal (right before seizure onset) and interictal period (time between two seizures). The interictal period is chosen from control data where seizure activity is not seen for at least 12 hours.

4.5 HFO Analysis

Even though events are detected automatically by each detector. They are considered candidate events pending visual approval of the true events and rejection of false events by expert users and EEG analysts. For this reason, we used examples presented in Navarrete et al. (2016) as reference for classifying the HFOs. Criteria used includes (1) minimum 4 oscillations that stand out from the background (Navarrette et al., 2016; Zelmann et al., 2012; Zelmann et al., 2014; Pail et al., 2013; Worrell et al., 2012); (2) duration of at least 25ms (de la Prida et al., 2015; Zelmann et al., 2012); and (3) power bump in spectra of the signal – wide enough in time and limited in frequency (Zelmann et al., 2012; Roehri N et al., 2017). Since our data was downsampled to a 1250Hz sampling rate, the frequency of interest was 80-625Hz. Figure 4.3-4.8 shows accepted and rejected events in our signal.

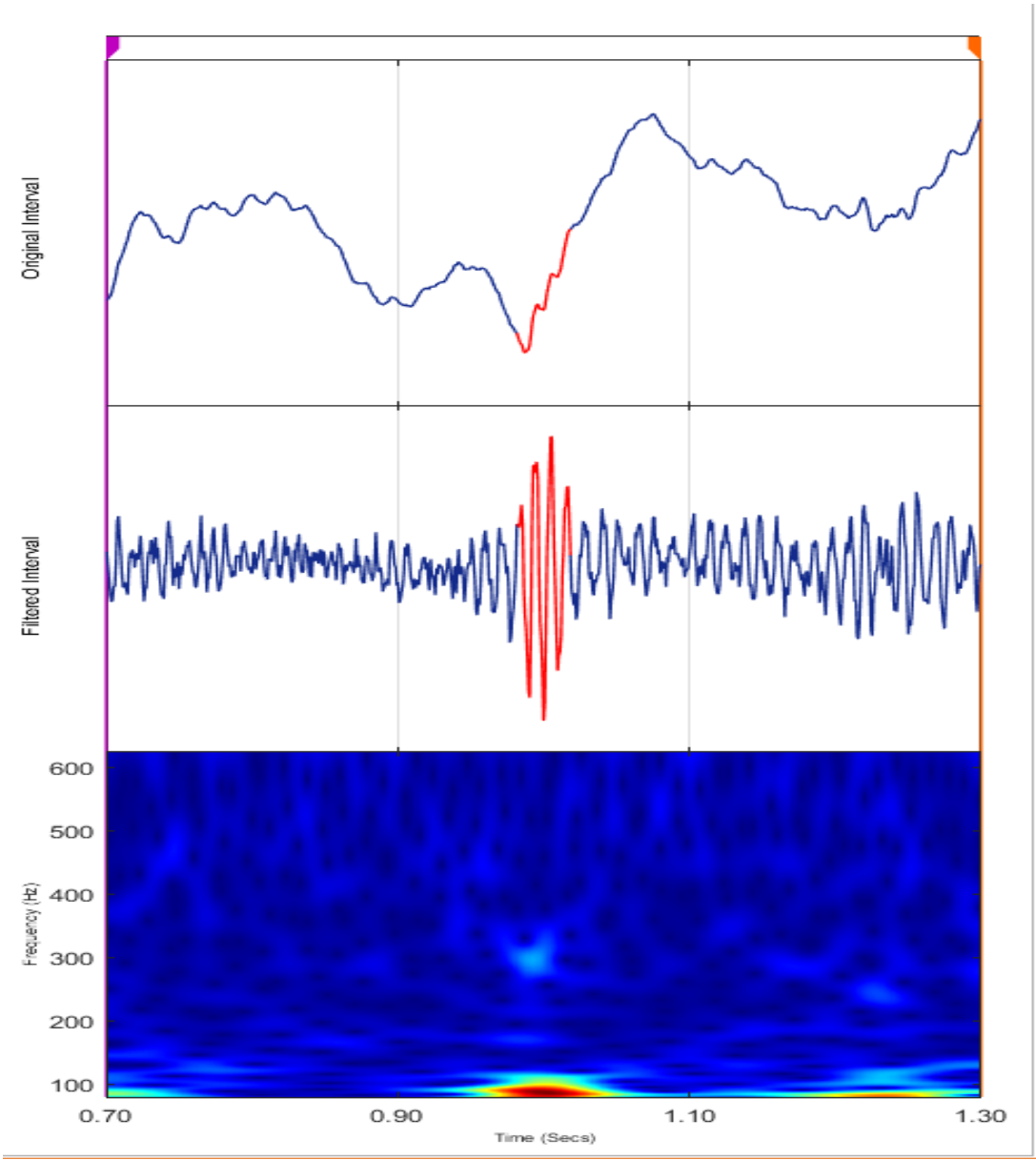

Figure 4.3 Accepted event – gamma

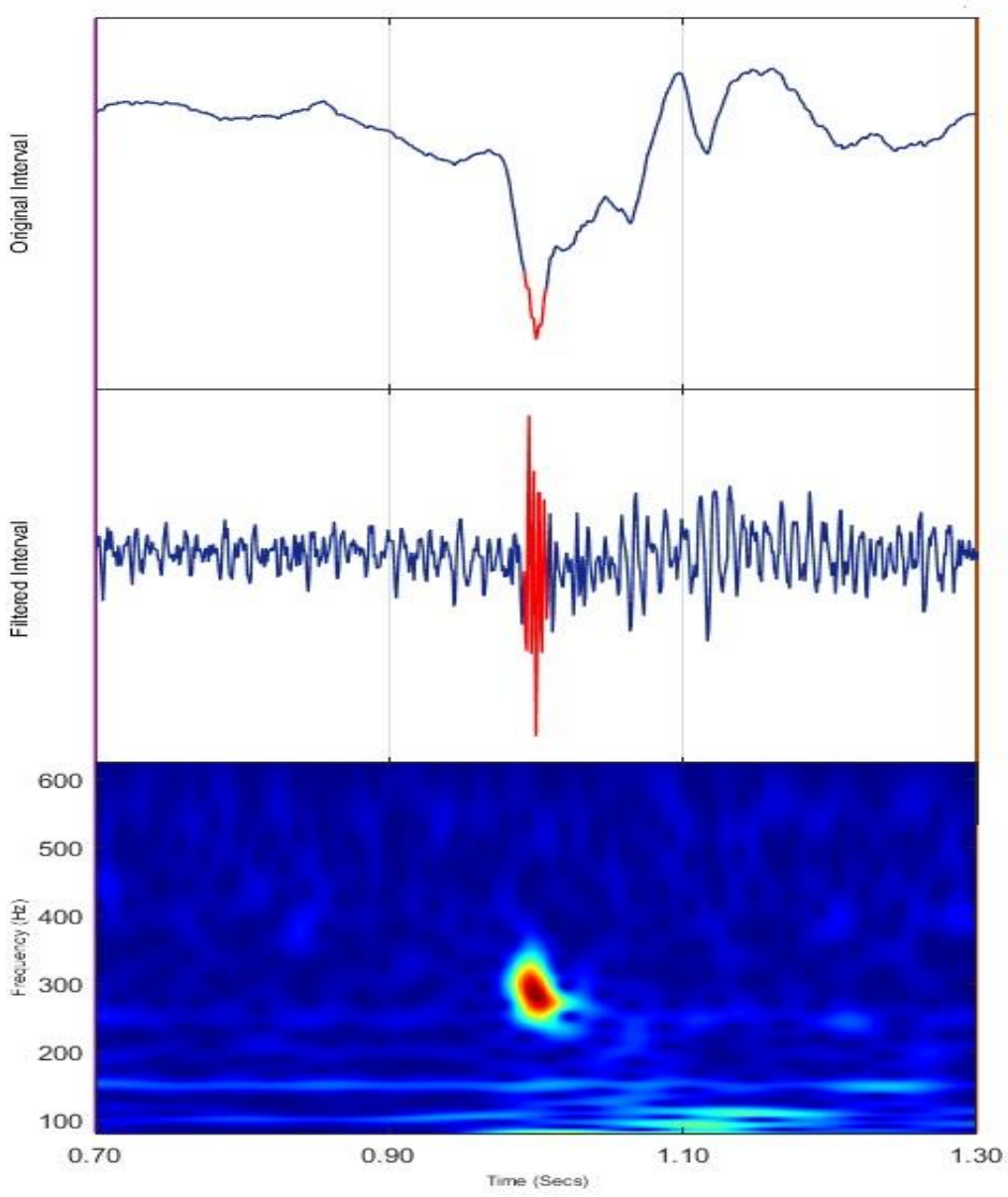

Figure 4.4 Accepted event- Fast Ripple

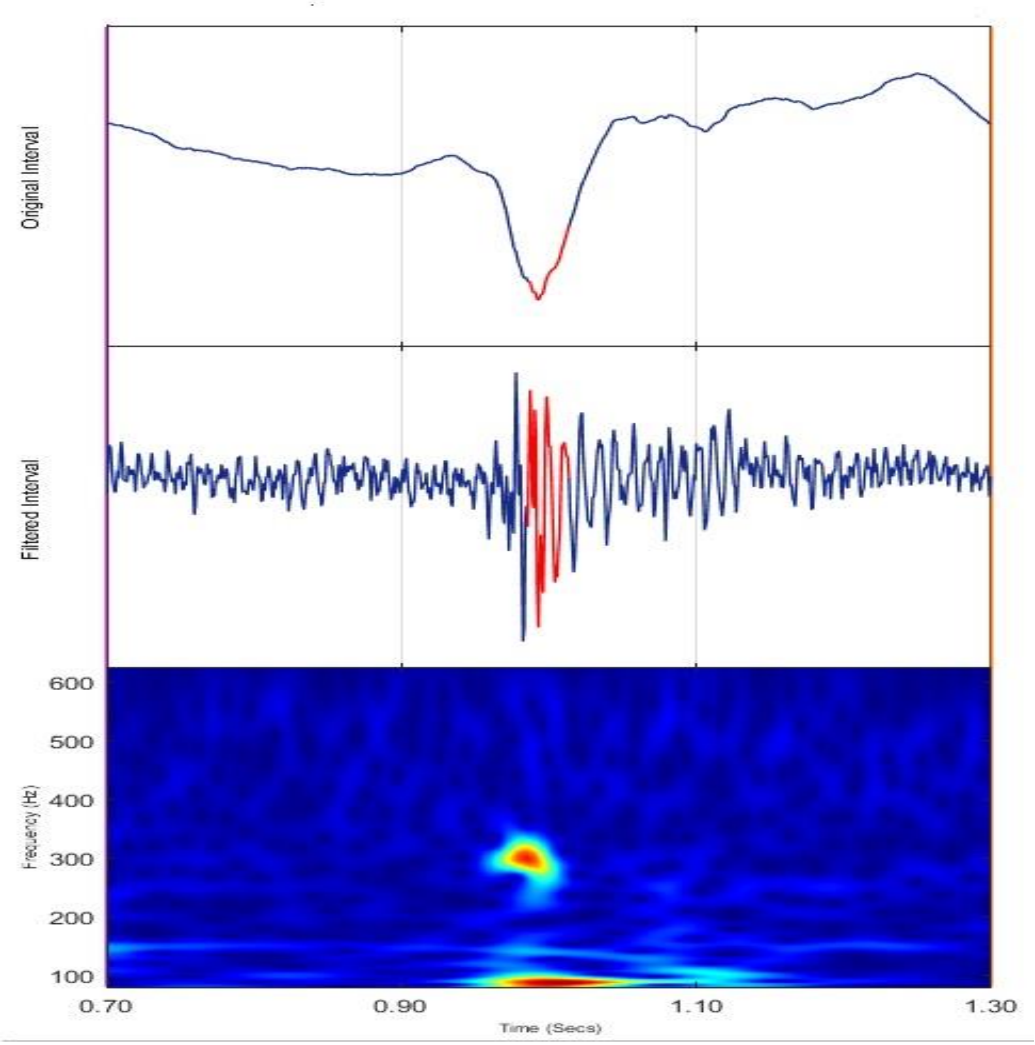

Figure 4.5 Accepted event- Ripple and Fast Ripple

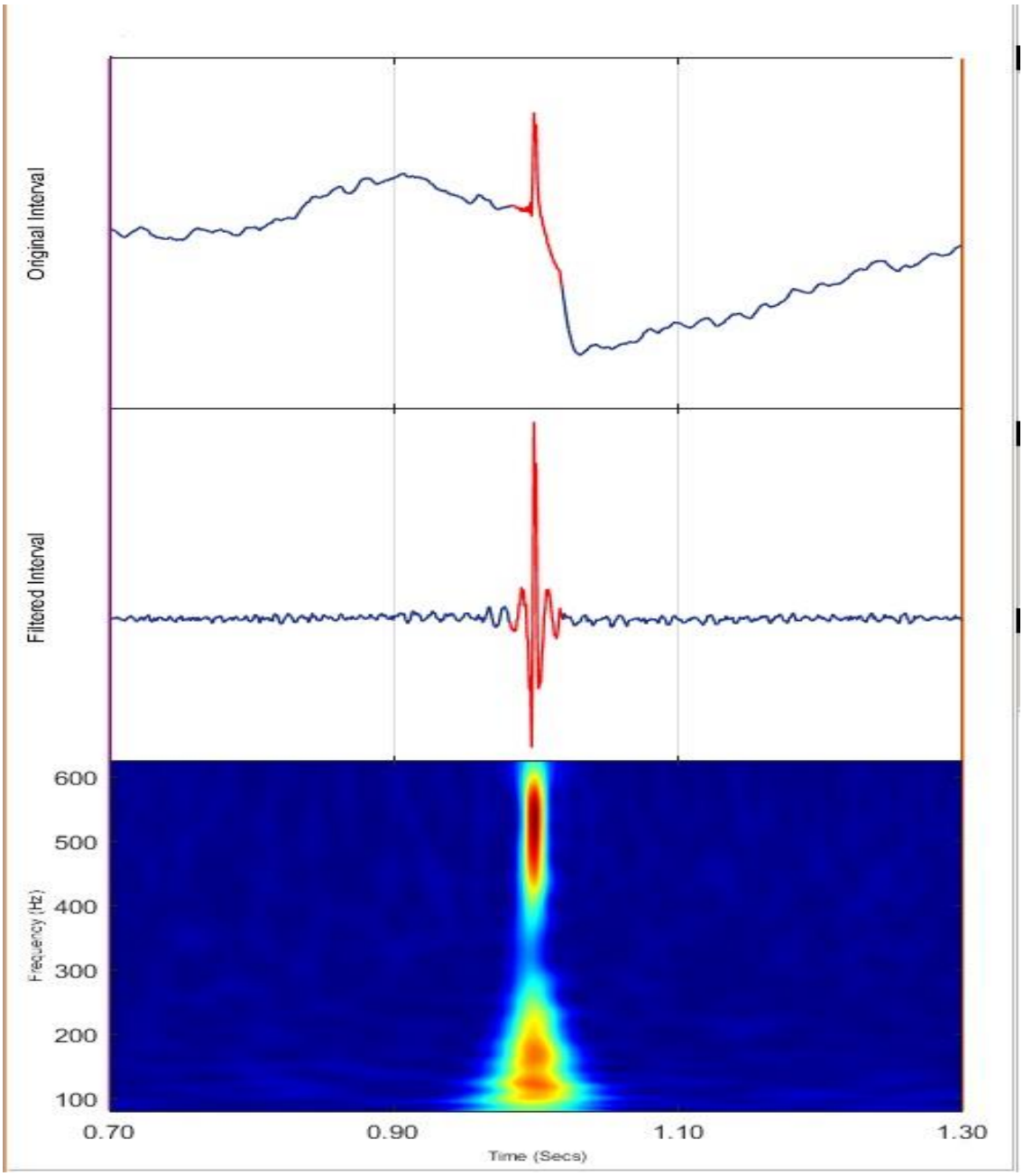

Figure 4.6 Denied event – Signal artifact due to spectral leakage

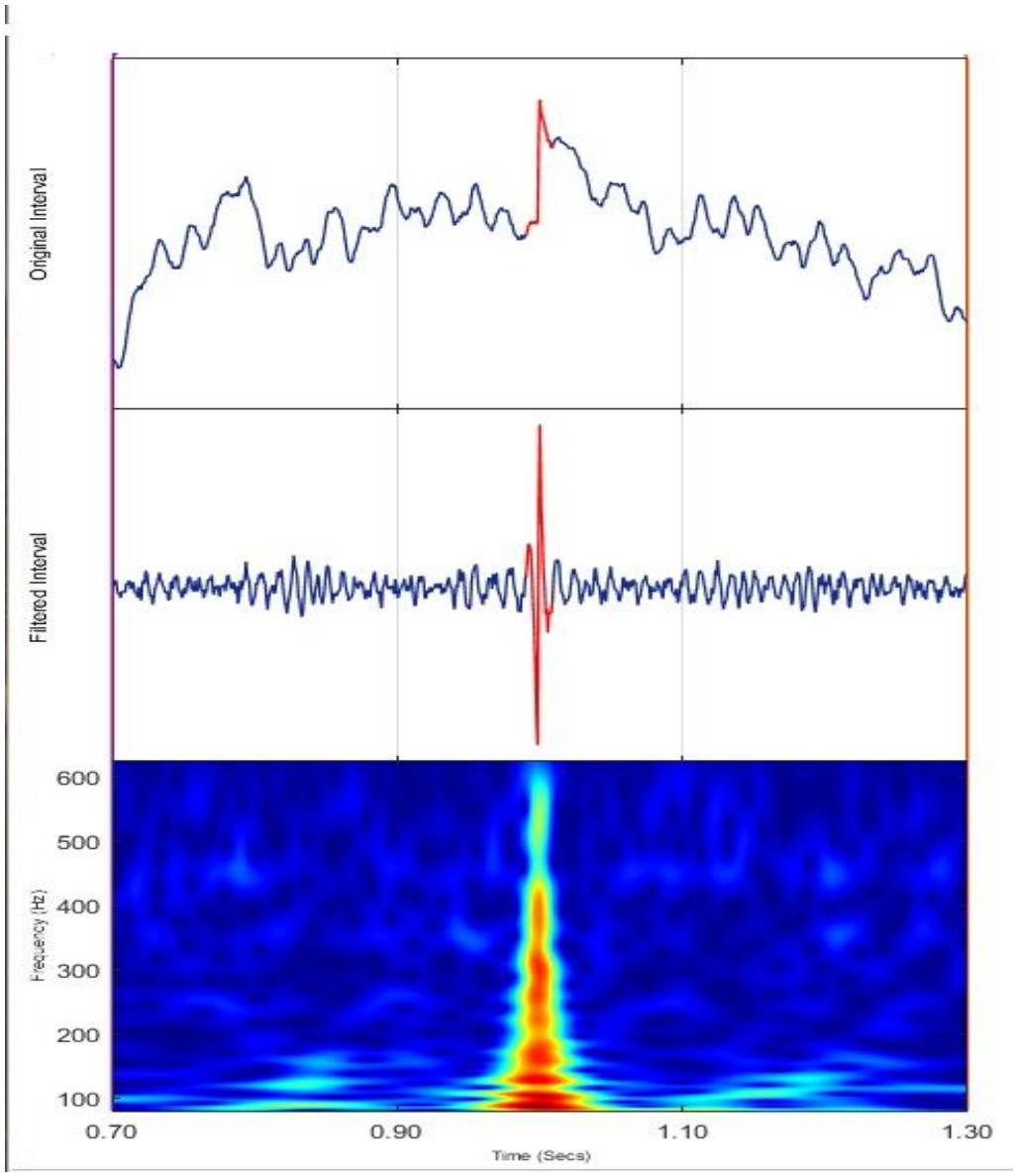

Figure 4.7 Denied event- Spike artefact due to filtering

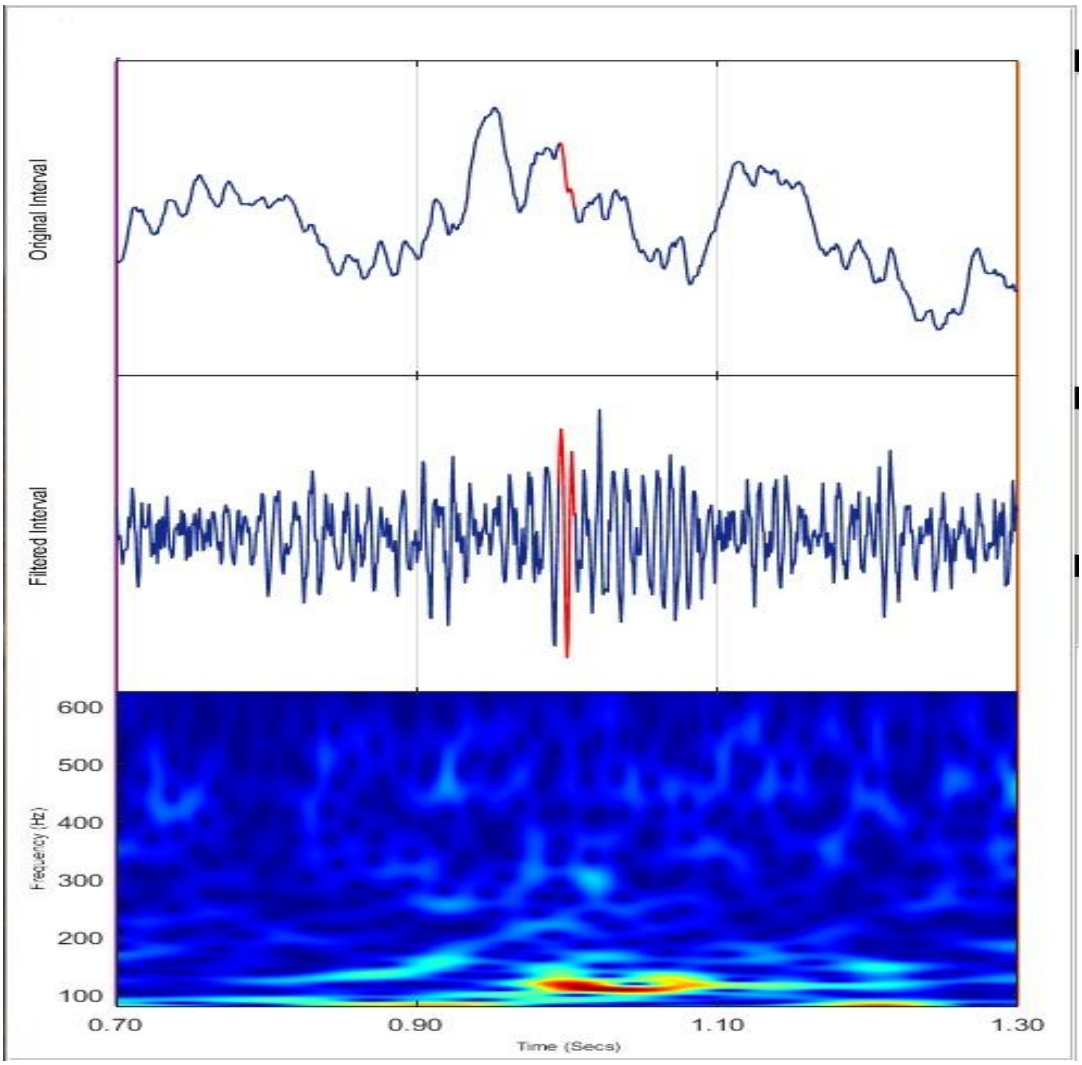

Figure 4.8 Denied event- Too similar to the background signals

4.6 HFO classification using Alexnet

As a final step in our work, we used deep learning as an exploration tool to evaluate it as a method for candidate HFO event classification. Alexnet, as discussed in Chapter 2, was used to classify the HFO events. For this purpose, we used the spectrogram (time-frequency plot) of the events. We classified the events into 4 categories – Ripple, Fast Ripple, Ripple and Fast ripple and Not HFO. Here, we used the default network of Alexnet to train and test our data. About 700 images of size 227x227x3 were used. Approximately, 720 images were used for training and testing. While conducting transfer learning, we augmented the collection of original images by applying random reflections in the left and right directions, horizontal and vertical translations, and noise thus expanding our dataset in order to prevent overfitting. Before training the network with transfer learning, we loaded the pretrained network and replaced the final layers to learn specific features to our dataset and reduced the number of classes from 1000 to 4. The algorithm then classifies validation images using the fine-tuned network. With feature extraction, we use the activations on the fully connected layer 'fc7' and use the features extracted from the training images to be predictor variables and train an SVM to classify the validation images. The Figure 4.9-4.12 shows the labels used for spectrograms.

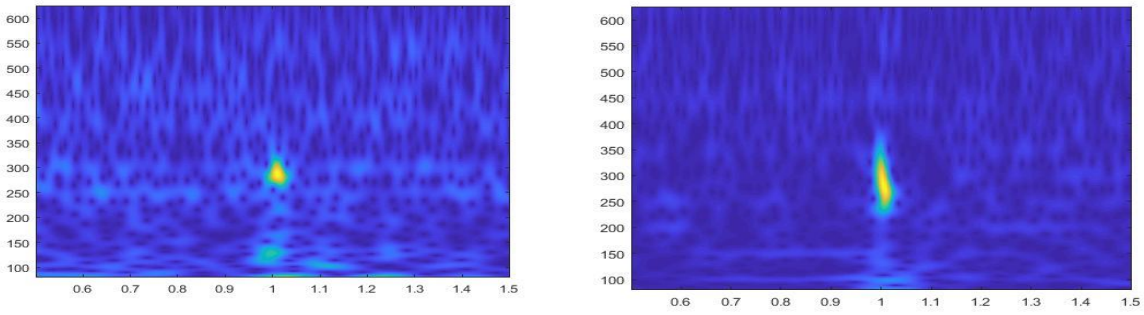

Figure4.9 Spectrogram labeled as Fast Ripple

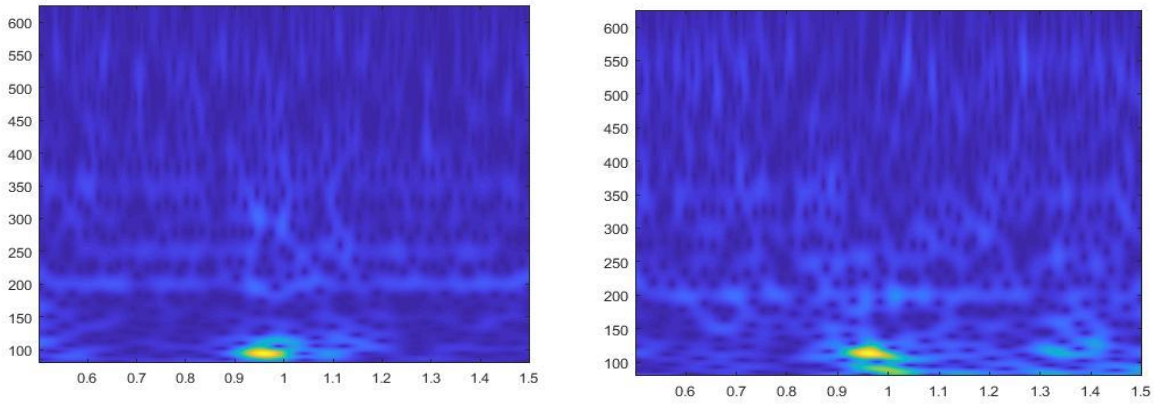

Figure 4.10 Spectrogram labeled as Ripple

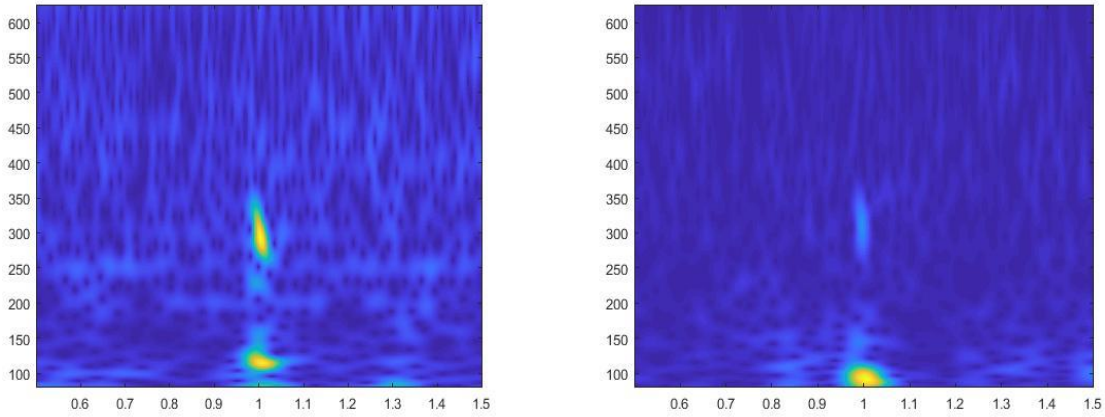

Figure 4.11 Spectrogram labeled as Fast Ripple and Ripple

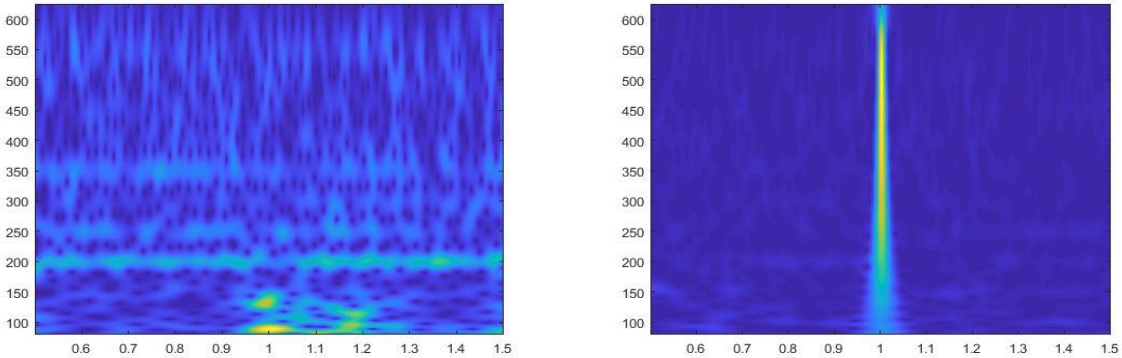

Figure 4.12 Spectrogram labeled as Not HFO

Chapter 5

Experiments

We performed 3 studies in our work. Our first work was the continuation of previous work by Kern BD (et al. 2016). Next with more patient specific data, we chose the electrodes that were marked as seizure origin as discussed in Chapter 3. Finally, a study using Alexnet for classification of the events.

5.1 Study 1- MNI and STE detection in 40 preictal minutes

At the beginning of our work we did not have enough patient specific data and used the work by (Kern B.D. et al., 2016) as our basis. In it, the condition of the patient was assumed to be focal epilepsy. It used an energy threshold method to identify the electrodes closer to the SOZ and it identified the first 5 electrodes crossing the threshold to be electrodes as likely to be the closest to the SOZ. In this work we chose the same electrodes. The previous work had data 20-min before the seizure but here we chose 40-min (except for seizure 4 which happened only 1.2 min after seizure 3) before the seizure and passed it through MNI and STE detectors. We manually selected the HFOs from the candidate events. We saw that even though MNI detects a greater number of candidate events, it sometimes misses some of the events. Table 5.1 shows this analysis. The numerator values in the tables refer to the total number of true HFOs and the denominator refers to the total number of candidate events detected in 40-min preictal data. The common column numbers are included in the total numbers per detector.

Table 5.1. HFO Rates from MNI and STE detectors for all seizures

Seizure 1	MNI	STE	Common in both
B6	46/90	24/35	14/32
B7	48/130	39/60	28/38
B8	10/40	2/11	1/7
D7	49/80	16/32	15/24
F2	99/182	78/95	62/71

Seizure 2	MNI	STE	Common in both
B6	56/102	45/60	35/39
B7	73/135	63/84	43/45
B8	17/41	16/27	9/11
D7	60/120	43/53	33/38
F2	131/201	139/155	38/53

Seizure 3	MNI	STE	Common in both
B6	64/156	47/82	33/53
B7	95/214	68/137	39/67
B8	35/119	23/56	18/42
D7	81/197	49/92	41/74
F2	191/956	113/177	72/110

Seizure 4	MNI	STE	Common in both
B6	20/42	1/9	1/9
B7	20/35	1/9	1/8
B8	16/36	0/6	0/6
D7	16/38	1/8	0/7
F2	24/45	0/5	0/5

Seizure 5	MNI	STE	Common in both
B6	41/100	24/36	19/25
B7	80/96	42/55	31/33
B8	21/52	9/21	6/9
D7	67/137	31/37	23/26
F2	96/179	53/145	46/69

Seizure 6	MNI	STE	Common in both
B6	32/105	18/28	13/20
B7	86/198	47/141	35/74
B8	14/94	9/15	5/7
D7	51/121	25/34	19/23
F2	80/144	77/104	55/67

Seizure 7	MNI	STE	Common in both
B6	47/103	23/33	13/30
B7	64/180	51/71	28/54
B8	10/42	2/10	2/9
D7	50/96	17/30	16/26
F2	102/268	82/119	62/110

Seizure 8	MNI	STE	Common in both
B6	58/117	45/64	35/49
B7	75/184	63/107	43/80
B8	21/76	18/33	11/24
D7	61/122	44/61	34/47
F2	142/365	144/164	58/63

Seizure 9	MNI	STE	Common in both
B6	107/214	60/76	52/61
B7	161/293	90/108	79/89
B8	34/83	19/24	13/18
D7	114/214	42/53	31/38
F2	113/236	81/100	67/75

5.2 Study 2-Detection in multiple SOZs

While we were working assuming the patient to have focal epilepsy, we received patient specific data as discussed in Chapter 3. So, we hypothesized after analyzing the table 3.1 that the patient suffered from generalized epilepsy and had multiple SOZs. We used the electrodes indicated as the origin in Table 4.1 to be the SOZs for each seizure respectively. 40-min of these electrodes immediately before seizure onset where passed into the MNI and STE detector and we repeated the work as described in the study 1. Here we neglected seizure 4 data as it happened only 1.2 min after seizure 3. Also, FBA3 and FBA4 electrodes for seizure 3 were dropped from the analysis as they showed the least activity. The Table 5.2 shows the number of HFOs identified in these electrodes for each seizure, respectively. The numerator values in the tables refer to true HFOs and the denominator refers to total number of candidate events detected in 40-min preictal data.

Table 5.2 HFO rates for channels indicated as seizure origin for all seizures in Table 4.1

Seizure 1	MNI	STE	Common in both
B6	56/102	45/60	35/39

Seizure 2	MNI	STE	Common in both
B5	26/206	6/25	6/25
C4	5/38	0/15	0/15

Seizure 3	MNI	STE	Common in both
A6	9/136	2/31	2/28
B5	47/318	8/64	7/49
B6	64/156	47/82	33/53
C4	7/142	2/35	2/30
C5	14/233	4/42	3/39
C6	14/164	4/48	4/39

Seizure 5	MNI	STE	Common in both
H1	14/73	3/7	3/7

Seizure 6	MNI	STE	Common in both
F2	85/144	77/104	55/67

Seizure 7	MNI	STE	Common in both
A5	5/40	0/3	0

Seizure 8	MNI	STE	Common in both
A6	3/11	2/5	2/5

Seizure 9	MNI	STE	Common in both
G3	9/61	10/20	4/20
H3	22/81	5/15	5/15

5.3 Study 3- Event classification with deep neural network

In this study, we made an attempt to classify the events using their spectrograms in Alexnet as discussed in Chapter 4. In Alexnet we used the feature extraction method, where the convolution network is used to extract features and an SVM classifier is used to classify the events. We divided the dataset into four learning categories: Fast ripple, not HFO, ripple, ripple and fast ripple. In total we have 720 images in the dataset that have been augmented in the algorithm to prevent overfitting. We split the dataset randomly into 70% of training data and 30% of test data.

Discussion

The study-3 event classification with a deep neural network was preliminary work with deep learning - a first attempt to try to eliminate visual verification of true HFO events from the candidates obtained with the automatic detectors. We used four classifications (Not HFO,

Ripple, Fast Ripple, Ripple and Fast Ripple) with 333 images, 313 images, 13 images, and 62 images per classification, respectively. We obtained accuracy of 60-80% with randomly split training and testing datasets. As this is just an exploration of deep learning viability in event classification, further study is to be made in order to eliminate time consuming visual verification processes.

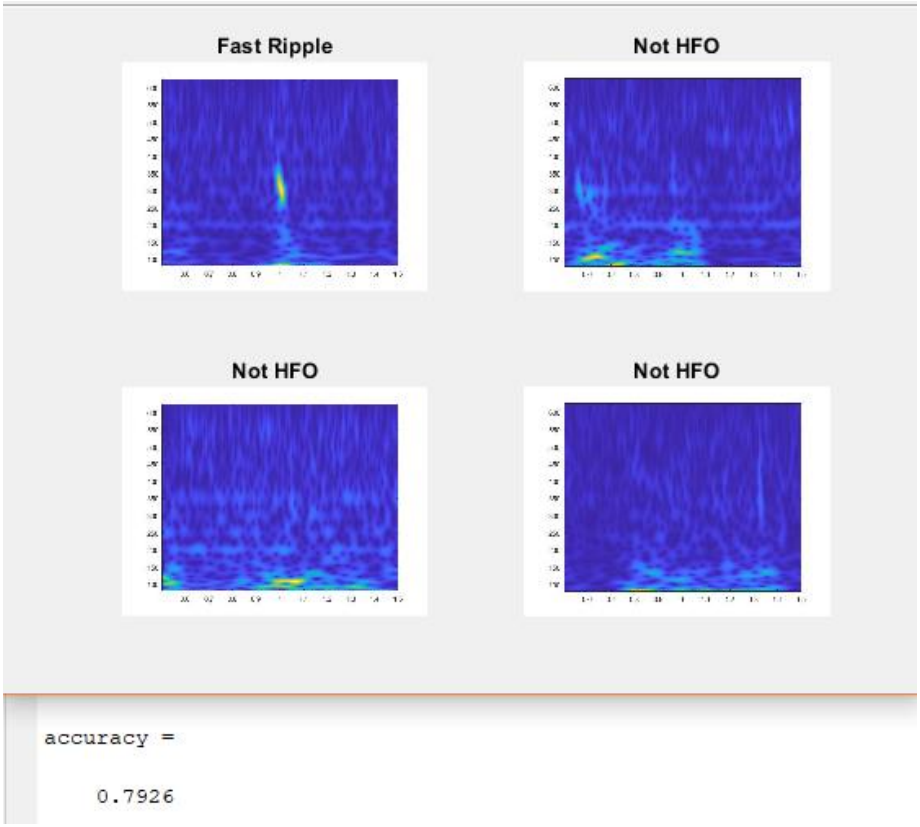

Figure 5.1 HFO classification using Alexnet

Chapter 6

Results

We obtained two different sets of results for study 1 and 2. In study 1, the electrodes chosen showed more activity than the electrodes indicated as the seizure origin from Table 4.1. We also found that the number of detected HFOs were higher in the preictal 20-min for this patient data.

In study 1, we found that in general, the MNI detector detected more HFOs and candidate events per electrode than the STE detector. Since each detector uses a different density function and threshold, depending on the patient and data used, we may get different results from these in future experiments. Notice that even though the STE detector has the lowest number of HFOs and candidate events, they are greater than the respective numbers in the common column. Thus, HFOs and candidate events detected by the STE method is not a subset of those found with the MNI detector.

Table 6.1 Average HFOs additional to common in MNI and STE detectors of all seizures

	Av.MNI	Av.STE	Av.Common in both
B6	27.34	8	23
B7	44.45	18	33.56
B8	12.56	3.67	7.23
D7	37.23	6.23	23.56
F2	55.89	32.23	46.89

Av.MNI = (MNI true events for each electrode) – (Common in both true events)

Av.STE = (STE true events for each electrode) – (Common in both true events)

Av.Common in both = average of all common true events for each electrode

While in study 2, almost all STE events were detected in MNI too due to the presence of a smaller number of true events out of candidate events. However, since most of the research work is based on focal epilepsies, it is hard to say whether the electrodes chosen here are right for consideration as the SOZ electrodes. In this study, we found again that in general, the MNI detector detected more events than the STE detector.

Table 6.2 Average HFOs additional to common events in MNI and STE detectors of all electrodes in Table 4.1

Seizure 1	MNI	STE	Common in both
B6	21	10	35

Seizure 2	MNI	STE	Common in both
B5	20	0	6
C4	5	0	0

Seizure 3	MNI	STE	Common in both
A6	7	0	2
B5	40	1	7
B6	31	14	33
C4	5	0	2
C5	11	1	3
C6	10	0	4

Seizure 5	MNI	STE	Common in both
H1	11	0	3

Seizure 6	MNI	STE	Common in both
F2	30	22	55

Seizure 7	MNI	STE	Common in both
A5	5	0	0

Seizure 8	MNI	STE	Common in both
A6	1	0	2

Seizure 9	MNI	STE	Common in both
G3	5	6	4
H3	17	0	5

We also found that for this patient data, the HFO activities were more in the 20-min immediately before seizures out of 40-min preictal signals.

Conclusion and Future work

We used F-scores to analyze and validate our results with study-1 data to support our conclusions about detector performance – results of the preliminary study on HFO classification with deep learning were not analyzed any further. We computed F-scores of MNI, STE, MNI union STE (MNI $\cup$ STE) and MNI intersection STE (MNI $\cap$ STE) for all seizures except seizure 4, this result was not used as it had only 140s of interictal period compared to other seizures. From the Figure 6.1and 6.2 (presented for study 1 and (MNI $\cap$ STE) as M&S and (MNI $\cup$ STE)as M$\cup$S), we notice that (MNI $\cup$ STE) performs better than the other choices – in both by seizure perspective and by electrode perspective. And (MNI $\cap$ STE) performs the worst. Considering MNI and STE by themselves, you will notice there is no single detector consistently performing better than the other for all seizures and all electrodes. The fact that (MNI $\cup$ STE) performs better than MNI by itself and that STE tends to be unpredictable, maybe due to its smaller

event counts, indicates that using (MNI ∪ STE) is the best choice for HFO detection. Given each detector contribution to the true HFO count, using more than one detector will be expected to enhance overall quality and also experimenting with additional detectors will help to identify a robust combination of detectors for automatic HFO detection.

Though our work shows promising results to consider combinations of detectors for our data, this needs to be verified with more data to obtain robust results for seizure prediction. Also, this may help robust identification of HFOs that might be part of physiological or pathological activities.

Many HFO detectors have been developed using different thresholding techniques and parameters. Their assumptions are due to the absence of a commonly accepted gold standard for HFO definition and statistical distribution analysis of the EEG signals. A recent study (Jard N. et al., 2017) suggests a global thresholding method to classify HFOs. In this, abrupt changes in the mean energy of a signal are considered to set the threshold to detect the candidate events. This method can be used as another detection algorithm to see how detection of HFO events varies.

Automatic detectors perform detection of candidate events, but the acceptance or rejection of events as HFOs is manually performed by experts and it is a time-consuming, inconsistent process. These are reasons for us to work with deep learning for HFO classification.

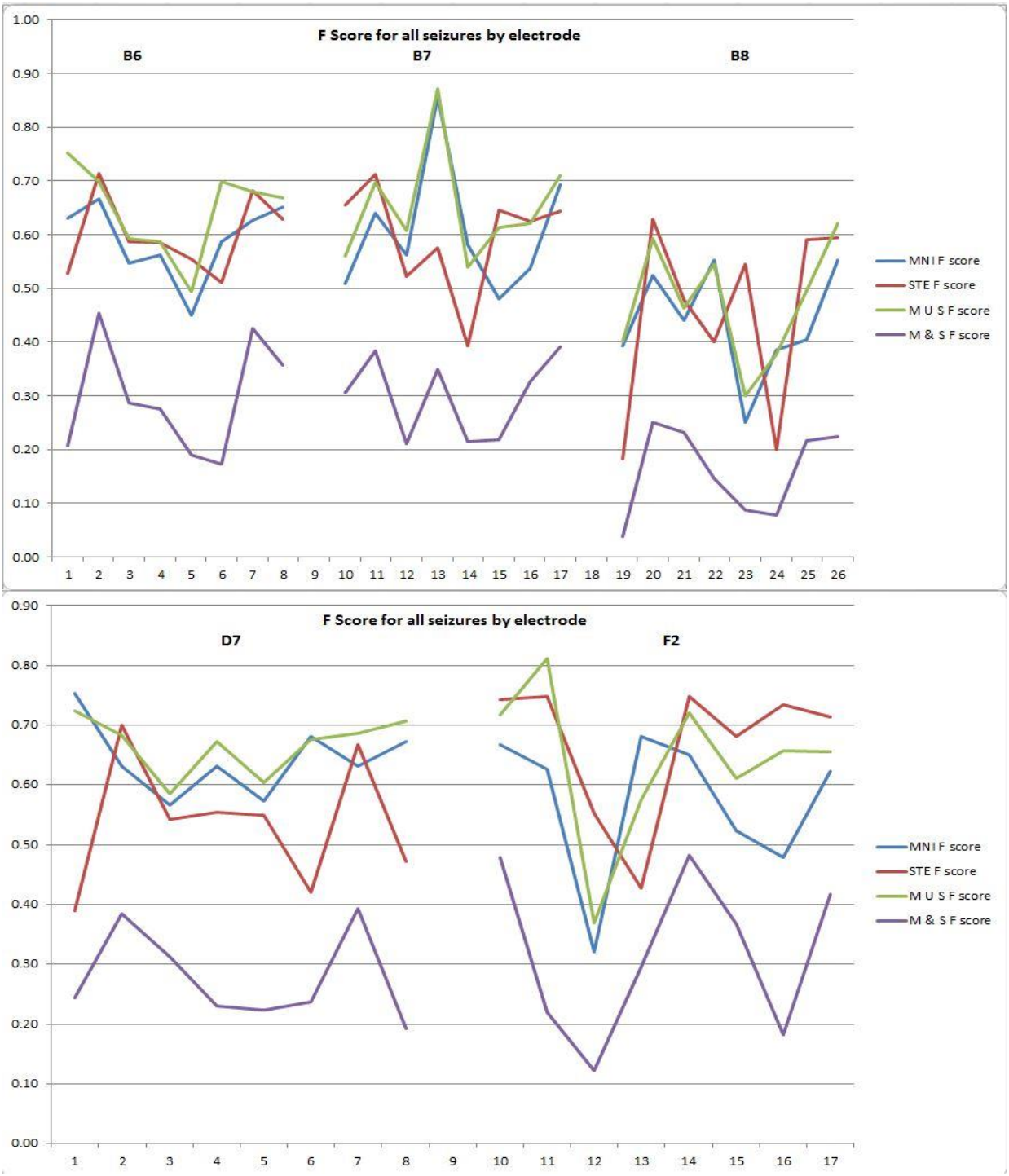

Figure 6.1 F-score of electrodes for study 1

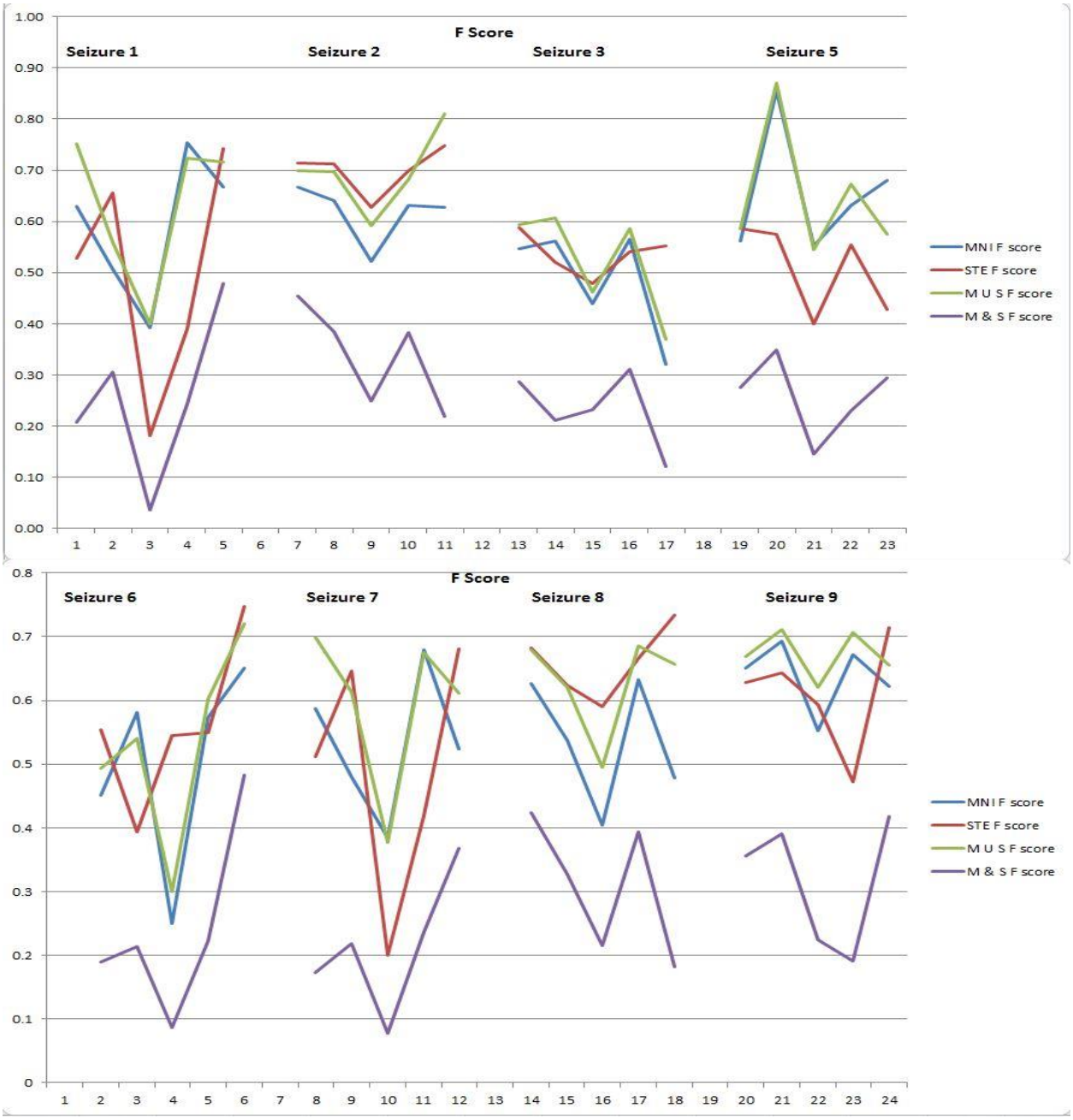

Figure 6.2 F-score of seizures for study 1

References

[1] Crépon B, Navarro V, Hasboun D, Clemenceau S, Martinerie J, Baulac M. 2010 Mapping interictal oscialltions greater than 200Hz recorded with intracranial macroelectrodes in human epilepsy. *Brain* 133:33-45

[2] de al Prida, L. M., Staba, R. J. and Dian J. A., 2015. Condundrums of high-frequency oscillations(80-800Hz) in the epileptic brain. Journal of clinical neurophysiology: official publication of the *American Electroencephalographic Society*,32(3), pp. 1-7.

[3] Fedele T, Burnos S, Boran E, Krayenbuhl N, Hilfiker P, Grunwald T., Sarthein J., 2017. Resection of high frequency oscillations predicts seizure outcome in the individual patient. *Scientific Reports*,

[4] Gardner AB, Worrell GA, Marsh E, Dlugos D, Litt B.2007 Human and automated detection of high-frequency oscillations in clinical intracranial EEG recordings. *Clin Neurophysiol* 118:1134-43

[5] Gloss D., Nolan S. J., Staba R., 2014. The role of high-frequency oscillations in epilepsy surgery planning. *Cochrane Database Syst Rev*,15(1), CD010235.

[6] Gotman J., Pariya Salami., Lėvesque M., Avoli M., 2012, A comparison between automated detection methods of high-frequency oscillations(80-500Hz) during seizures. *Journal of Neuroscience Methods* 211(2012) 265-271

[7] Jacobs J, Zijlmans M, Zelman R, 2010. Value of electrical stimulation and high frequency oscillations(80-500Hz) in identifying epileptogenic areas during intracranial EEG recording. *Epilepsia* 51:573-582.

[8] Jard N., Kachenoura A., Nica A., Merlet I., Wendling F., 2017. A Page-Hinkley based method for HFOs detection in epileptic depth-EEG. *25th European Signal Processing Conference (EUSIPCO),* pp. 1295-1299.

[9] Kucewicz MT, Cimbalnik J, Matsumoto JY, Brinkmann BH, Bower MR. Vasoli V, Sulc V, Meyer F, Marsh WR, Stead SM, Worrel GA,2014. High frequency oscillations are associated with cognitive processing in human recognition memory. *Brain* 137(8):2231-2241

[10] Kern, BD, "The viability of high-frequency oscillation analysis in EEG signals for seizure prediction" (2016). *ETD Collection for University of Texas, El Paso*. AAI10249766.

[11] Krizhevsky A, Sutskever I, Hinton GE., 2012. ImageNet Classification with Deep Convolutional Neural Networks.*Advances in Neural Information Processing Systems*. pp 1097-1105

[12] Kay, S., 2006. Intuitive probability and random processes using MATLAB®. *Springer Science & Business Media.*

[13] Karoly PJ, Freestone DR, Boston R, Grayden DB, Himes D, Leyde K, Seneviratne U, Berkovic S, Brien TO, Cook MJ., 2016, Interictal spikes and epileptic seizures: their relationship and underlying rhythmicity. *Brain* 139:1066-1078

[14] Laura Sanders. Brain waves may focus attention and keep information flowing. *Science News*,2013. https://www.sciencenews.org/article/brain-waves-may-focus-attention-and-keep-information-flowing.

[15] Li S, Zhou W, Yuan Q, Liu Y., 2013. Seizure prediction using spike rate of intracranial EEG. *IEEE Transactions on Neural Systems and Rehabilitation Engineering 21*, 880-886.

[16] Mormann, F., Andrzejak, R.G., Elger, C.E. and Lehnertz, K., 2007. Seizure prediction: the long and winding road. *Brain*, *130*(2), pp.314-333.

[17] Navarrete M, Rojas CA, Quyen MLV, Valderrama M., 2016. RIPPLELAB: A Comprehensive Application for the Detection, Analysis and Classification of High Frequency Oscillations in Electroencephalographic Signals. *PLos ONE* 11(6): e0158276

[18] Proakis, J.G., 2001. Digital signal processing: principles algorithms and applications. *Pearson Education India.*

[19] Pail, M., Halámek, J., Daniel, P., Kuba, R., Tyrlíková, I., Chrastina, J., Jurák, P., Rektor, I. Brázdil, M., 2013. Intracerebrally recorded high frequency oscillations: simple visual assessment versus automated detection. *Clinical Neurophysiology*, *124*(10), pp.1935- 1942.

[20] Roehri N., Pizzo F., Lagarde S., Lambert I., Nica A, McGonigal A., Giusiano., Bartolomei F., Bėnar CG.2018. High-frequency oscillations are not better biomarkers of epileptogenic tissues than spikes. *Ann Neurol*;83(1):84-97

[21] Roehri N., Pizzo F., Bartolomei F., Bėnar CG., Wendling F., 2017. What are the assets and weaknesses of HFO detectors? A benchmark framework based on realistic simulations. *PLOS ONE* 12(4): e0174702

[22] Sengupta N., McNabb CB., Kasabov N., Russell BR., 2018. Integrating Space,Time and Orientation in Spiking Neural Networks: A Case Study on Multimodal Brain Data Modeling. *IEEE Transactions on neural Networks and Learning systems*,99, pp. 1-15.

[23] Staba RJ, Wilson CL, Bragin A, Fried I, Engel Jr J.2002 Quantitave analysis of high frequency oscillations(80-500Hz) recorded in human epileptic hippocampus and entorhinal cortex. *Neurophysiol* 88,pp. 1743-52.

[24] Teixeira C.A., Direito B., Drentrup HF., Valderrama M., Costa RP., Rojas CA, Nikolopoulos S., Quyen LM., Timmer J,Schelter B., Dourado A,2011. EPILAB:A software package for studies on the prediction of epileptic seizures. Journal of Neuroscience Methods;200(2011),pp. 257-271

[25] Tatum IV, W.O., 2014. Handbook of EEG interpretation. *Demos Medical Publishing*.

[26] Worrell GA., Jerbi K., Kobayashi K., Lina JM, Zelman R., Le Van Quyen M., 2012. Recording and analysis techniques for high-frequency oscillations. *Progress in neurobilology*,98(3),pp. 265-278.

[27] Zijlmans, M., Jiruska, P., Zelmann, R., Leijten, F.S., Jefferys, J.G. and Gotman, J., 2012. High-frequency oscillations as a new biomarker in epilepsy. *Annals of neurology*, *71*(2), pp.169-178.

[28] Zelmann R., Jacobs J., Jirsch J., Chander R, Claude- Édouard Châtillon, Dubeau F, and Gotman J., 2009. High frequency oscillations(80-500Hz) in the preictal period in patients with focal seizures, *Epilepsia*,50(7):1780-1792.

[29] Zelmann, R., Mari, F., Jacobs, J., Zijlmans, M., Dubeau, F. and Gotman, J., 2012. A comparison between detectors of high frequency oscillations. *Clinical Neurophysiology*, *123*(1), pp.106-116.

[30] Zelmann, R., Lina, J.M., Schulze-Bonhage, A., Gotman, J. and Jacobs, J., 2014. Scalp EEG is not a blur: it can see high frequency oscillations although their generators are small. *Brain topography*, *27*(5), pp.683-704

Vita

Deeksha Seetharama Bhat was born in Bengaluru, Karnataka, India. Graduated from Nitte Meenakshi Institute of Technology in 2016 with Bachelors in Electronics and Communication Engineering. She later decided to join The University of Texas at El Paso to pursue Master of Science in Electrical Engineering in 2016 . She graduated with M.S degree in Fall of 2018.

Contact Information: deeksha.bhat765@gmail.com

This thesis was typed by Deeksha Seetharama Bhat